American Mineralogist, Volume 93, pages 283–299, 2008

Boralsilite, $Al_{16}B_6Si_2O_{37}$, and "boron-mullite:" Compositional variations and associated phases in experiment and nature

Edward S. Grew,[1,*] Heribert A. Graetsch,[2] Birgit Pöter,[2] Martin G. Yates,[1] Ian Buick,[3] Heinz-Jürgen Bernhardt,[4] Werner Schreyer,[2,†] Günter Werding,[2] Christopher J. Carson,[3] and Geoffrey L. Clarke[6]

[1]Department of Earth Sciences, University of Maine, 5790 Bryand Research Center, Orono, Maine 04469-5790, U.S.A.
[2]Institut für Geologie, Mineralogie und Geophysik, Ruhr-Universität Bochum, D-44780 Bochum, Germany
[3]Research School of Earth Sciences, Australian National University, Canberra, ACT 0200, Australia
[4]Zentrale Elektronen-Mikrosonde, Institut für Geologie, Mineralogie und Geophysik, Ruhr-Universität Bochum, D-44801 Bochum, Germany
[6]School of Geosciences, University of Sydney, NSW 2006, Australia

Abstract

Boralsilite, the only natural anhydrous ternary B_2O_3-Al_2O_3-SiO_2 (BAS) phase, has been synthesized from BASH gels with Al/Si ratios of 8:1 and 4:1 but variable B_2O_3 and H_2O contents at 700–800 °C, 1–4 kbar, close to the conditions estimated for natural boralsilite (600–700 °C, 3–4 kbar). Rietveld refinement gives monoclinic symmetry, *C*2/*m*, a = 14.797(1), b = 5.5800(3), c = 15.095(2) Å, β = 91.750(4)°, and V = 1245.8(2) Å^3. Boron replaces 14% of the Si at the Si site, and Si or Al replaces ca. 12% of the B at the tetrahedral B2 site. A relatively well-ordered boralsilite was also synthesized at 450 °C, 10 kbar with dumortierite and the OH analogue of jeremejevite. An orthorhombic phase ("boron-mullite") synthesized at 750 °C, 2 kbar has mullite-like cell parameters a = 7.505(1), b = 7.640(2), c = 2.8330(4) Å, and V = 162.44(6) Å^3. "Boron-mullite" also accompanied disordered boralsilite at 750–800 °C, 1–2 kbar.

A possible natural analogue of "boron-mullite" is replacing the Fe-dominant analogue of werdingite in B-rich metapelites at Mount Stafford, central Australia; its composition extends from close to stoichiometric Al_2SiO_5 to $Al_{2.06}B_{0.26}Si_{0.76}O_5$, i.e., almost halfway to Al_5BO_9. Boralsilite is a minor constituent of pegmatites cutting granulite-facies rocks in the Larsemann Hills, Prydz Bay, East Antarctica, and at Almgotheii, Rogaland, Norway. Electron-microprobe analyses (including B) gave two distinct types: (1) a limited solid solution in which Si varies inversely with B over a narrow range, and (2) a more extensive solid solution containing up to 30% $(Mg,Fe)_2Al_{14}B_4Si_4O_{37}$ (werdingite). Boralsilite in the Larsemann Hills is commonly associated with graphic tourmaline-quartz intergrowths, which could be the products of rapid growth due to oversaturation, leaving a residual melt thoroughly depleted in Fe and Mg, but not in Al and B. The combination of a B-rich source and relatively low water content, together with limited fractionation, resulted in an unusual buildup of B, but not of Li, Be, and other elements normally concentrated in pegmatites. The resulting conditions are favorable in the late stages of pegmatite crystallization for precipitation of boralsilite, werdingite, and grandidierite instead of elbaite and B minerals characteristic of the later stages in more fractionated pegmatites.

Keywords: Boralsilite, "boron-mullite," werdingite, boron, pegmatite, Rietveld refinement, electron microprobe, Larsemann Hills, Antarctica, Almgjotheii, Norway

Introduction

The first anhydrous ternary phases to be synthesized in the system B_2O_3-Al_2O_3-SiO_2 (BAS) were poorly ordered high-temperature (930–1600 °C) orthorhombic materials related to mullite and restricted to a band of solid solution between 3:2 mullite ($Al_6Si_2O_{13}$) and $Al_{18}B_4O_{33}$ (Fig. 1; Letort 1952; Dietzel and Scholze 1955; Scholze 1956; Gelsdorf et al. 1958; Gielisse and Foster 1961). G. Werding, W. Schreyer, and their colleagues synthesized mullite-like orthorhombic compounds hydrothermally at geologically accessible temperatures (e.g., Werding and Schreyer 1996). The compositions of most of these materials could not be determined; an exception was the compound having the formula $Al_8B_2Si_2O_{19}$ and doubled a and c parameters compared to mullite (Werding and Schreyer 1992). However, the first ternary BAS phase to be discovered in nature, boralsilite, $Al_{16}B_6Si_2O_{37}$, is ordered and monoclinic, with all three cell parameters doubled (Grew et al. 1998a; Peacor et al. 1999). Armed with knowledge that an ordered compound had been discovered, Pöter et al. (1998) successfully synthesized under hydrothermal conditions a monoclinic compound having both the degree of order and the composition of natural boralsilite.

Nonetheless, the stability relationships and conditions of formation of boralsilite and the mullite-like compounds remain poorly understood. The objective of the present study is to re-examine synthetic boralsilite and mullite-like aluminoboro-

* E-mail: esgrew@maine.edu
† Deceased.

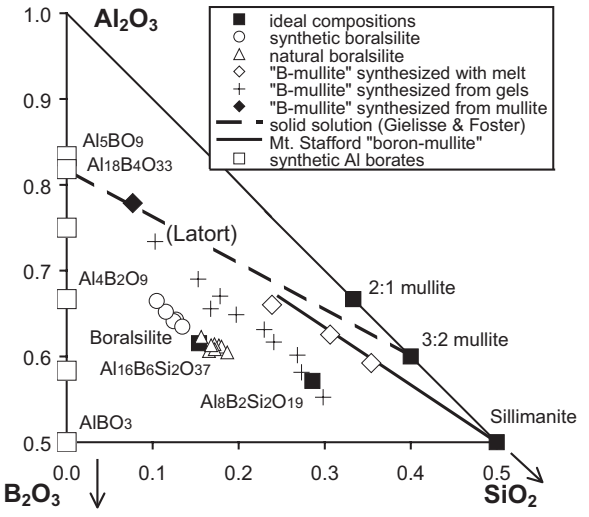

FIGURE 1. Plot in mol% of phases in the B_2O_3-Al_2O_3-SiO_2 system. Data on synthetic (Si < 2 per 37 O) and natural boralsilite (only compositions with Si > 2 per 37 O, sample 121501E) are taken from Figure 6. Gielisse and Foster (1961) confirmed the solid solution (dashed line) between $Al_{18}B_4O_{33}$ (A_9B_2) and $Al_6Si_2O_{12}$ (3:2 mullite), which had been suggested by the syntheses of "boron-mullite" from a 3:1 gel (Letort 1952), with melt (Dietzel and Scholze 1955), and from mullite (Gelsdorf et al. 1958). Other "boron-mullite" synthesized from gels (B4; W4) is taken from Figure 7. Solid solution in the Mount Stafford "boron-mullite" is based on the least-squares fits in Figure 9. Stoichiometries of binary Al borates are based on reported compositions (e.g., Scholze 1956; Gielisse and Foster 1962; Sokolova et al. 1978; Ihara et al. 1980; Garsche et al. 1991; Mazza et al. 1992); the number of discrete phases could be fewer than the six shown owing to solid solutions.

silicates and compare the synthetic compounds with naturally occurring analogues to better constrain their origin in nature and the conditions under which they formed. We refined the crystal structure of the synthetic boralsilite to determine whether it is as ordered as the natural material. During the 2003–2004 Antarctic field season, we collected specimens from nine boralsilite-bearing pegmatites and mapped the distribution of these pegmatites and associated B-enriched host rocks in the Larsemann Hills, the type locality for boralsilite. Additional insight on the origin of boralsilite and related compounds is provided by the discovery of a mullite-like boroaluminosilicate as a breakdown product of werdingite at Mount Stafford, central Australia (Buick et al. 2006).

Following Werding and Schreyer (1984, 1996), and for want of a better term, we refer to the synthetic and natural mullite-like orthorhombic ternary aluminum-borosilicates as "boron-mullite." The ferromagnesian solid solutions cordierite-sekaninaite, grandidierite-ominelite, and werdingite-Fe analogue of werdingite are referred to simply by the names of the Mg end-member throughout the paper, although these minerals are, for the most part, Fe-dominant in the B-rich metapelites from Mount Stafford and in the pegmatite from Almgjotheii.

ANALYTICAL METHODS

The synthetic and natural borosilicate compounds were analyzed with a Cameca SX-100 electron microprobe at the University of Maine using wavelength-dispersive spectroscopy (WDS). Analytical conditions were twofold at each spot: 5 kV accelerating voltage and 40 nA beam current for B; 15 kV accelerating voltage and 10 nA beam current for Mg, Al, Si, Ca, Ti, Mn, Fe, and As—the only constituents found above detection limits (except Ca) in these four borosilicates and dumortierite. The spot size for all elements ranged from 5 to 20 μm depending on grain size; a larger spot size was used if at all possible. Cameca's PeakSight software allowed for the cycling from one set of conditions to another. Samples were analyzed for B in peak-area mode with a Mo-B_4C (200 Å) synthetic crystal because the B peak is broad and asymmetrical (Fig. 2a); peak integration was carried out over 1000 steps, spanning wavelengths 60 to 78 Å. The upper and lower portions of this peak area were background and were regressed to determine the background contribution under the peak. The other constituents were measured in peak-height mode. Backgrounds for all constituents were measured at each analytical spot. We used the following minerals as standards: elbaite [B$K\alpha$, sample 98144, Dyar et al. (2001) using B from the crystal-structure refinement and the University of Maine electron microprobe analysis for the other constituents], diopside (Mg$K\alpha$, Ca$K\alpha$), kyanite (Al$K\alpha$, Si$K\alpha$), rutile (Ti$K\alpha$), rhodonite (Mn$K\alpha$), almandine (Fe$K\alpha$), and skutterudite (As$L\alpha$). Data were processed using the X-Phi correction of Merlet (1994).

B$K\alpha$ X-rays are typically difficult to quantify with the electron microprobe due to absorption, peak shifts, and interference with high-order spectra (McGee and Anovitz 1996). B$K\alpha$ measured on boralsilite using a 200 Å, Mo-B_4C crystal is asymmetric having 2.5 times higher background on the short-wavelength side of the B$K\alpha$ peak compared to the long-wavelength side. The background in the B$K\alpha$ interval increases markedly with SiO_2 content at wavelengths that would also affect the low wavelength side of the B$K\alpha$ peak (Fig. 2b). This interference is likely due to seventh- and eighth-order Si$K\alpha$ peaks and would affect the both the estimated background and the area under B$K\alpha$ peak in both standards and unknowns. Higher SiO_2 content of the standard compared to boralsilite and "boron-mullite" may lead to an over estimation of B_2O_3, but quantifying these interferences is difficult. Equally difficult to quantify is the impact of the peak at approximately 67 Å (Fig. 2b). This peak is unrelated to any specific interference and may be caused by fluorescence of B from the Mo-B_4C crystal (McGee and Anovitz 1996).

Prior to the analyses at the University of Maine, H.-J. Bernhardt carried out electron-microprobe analyses (EMPA) of the synthetic products for SiO_2 and Al_2O_3 using a Cameca SX-50 at the Ruhr-Universität Bochum. The data were corrected using a PAP matrix-correction procedure assuming that B_2O_3 is equal to the difference between the total and 100 wt%. The EMPA at the University of Maine gave SiO_2 and Al_2O_3 contents that fall largely within the ranges obtained at the Ruhr-Universität Bochum, but measurement of B_2O_3 brought the totals only to 67.1–80.5 wt% for disordered boralsilite and "boron-mullite." One explanation for this deficit could be water in the run products, but the analyzed grains did not decompose as expected if large amounts of H_2O had been present, although some showed a burn mark after long exposure to the electron beam. Instead, the appearance of the grains in the SEM images suggested that the analyzed grains are porous aggregates. In light of the study by Sorbier et al. (2004) showing that signal loss in mesoporous alumina (pore diameter <50 nm) resulted from epoxy soaked up during sample preparation, we suspected that the low totals resulted from an analogous contamination during preparation of the plug mounts. We performed the following three tests on one grain each of "boron-mullite" (B4) and ordered boralsilite (W2) at 15kV, 10 nA, with a focused beam: (1) counts per second (cps) of C$K\alpha$ for "boron-mullite" were five times greater than cps of C$K\alpha$ for ordered boralsilite (67 vs. 13 cps) and decreased with time after repeated analyses at one spot; (2) wt% totals for "boron-mullite" increased from 72 to 84% after repeated analyses at one spot, whereas totals for boralsilite remained unchanged; and (3) a trace of Cl was detected in WDS and energy dispersive spectroscopic (EDS) scans of "boron-mullite;" minor Cl was found in the epoxy in the plug. These observations can be explained by the presence of C in the contaminated grain in addition to that in the carbon coat and by volatilization of Cl-bearing epoxy under the electron beam. The repeated analysis at one spot on "boron-mullite" B4 resulted in a decrease in the proportion of B_2O_3 from 0.169 to 0.149, which exceeds the range in B_2O_3 obtained by repeated analyses of boralsilite W2, 0.236–0.243. This drift suggests contamination from the epoxy, but no B was detected in the epoxy used in the plug mount (detection limit estimated to be 0.25 wt% B_2O_3), and no B was reported in a chemical analysis supplied by the manufacturer of the epoxy. Whatever the cause of the drift in B_2O_3 contents, its effect appears not to be significantly greater than other uncertainties in the EMPA, and the data can provide some useful information on the compositions of disordered boralsilite and "boron-mullite."

The scanning electron microscope (SEM) images were obtained on a Cambridge stereoscan 250 MK3 instrument operated by Rolf Neuser at the Ruhr-Universität Bochum. The samples were sputtered-coated with gold.

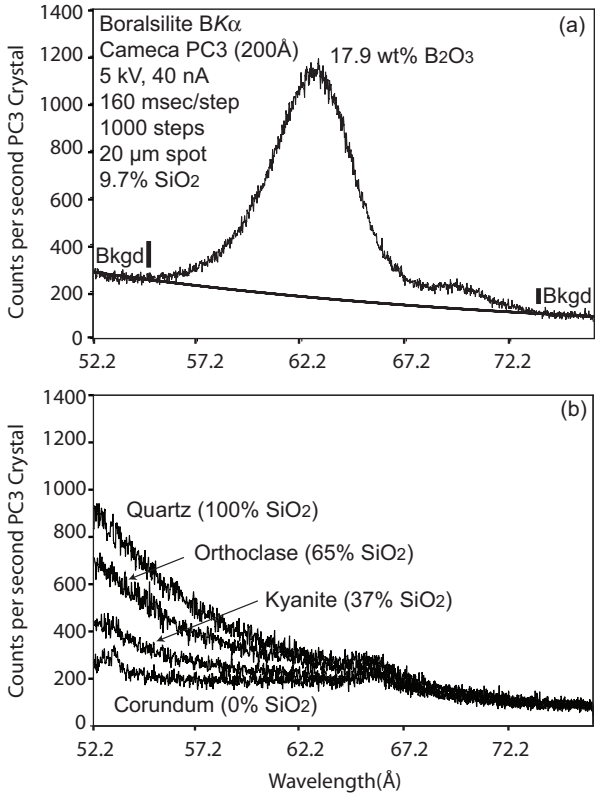

FIGURE 2. Traces of WDS scan of wavelengths where B*K*α peak is located. (**a**) Scan of boralsilite (sample 010602a1; grain 3). The measured peak area lies between the two vertical bars, beyond which is background. (**b**) Scans of minerals containing no B showing increase of background with increasing SiO_2 content.

Starting materials for the experiments in most cases were gels having an Al:Si ratio of 8:1 or 4:1 prepared from tetraethyl orthosilicate (TEOS) and Al powder dissolved in HNO_3 (diluted 1:1), then gelatinized with ammonia and heated to thoroughly decompose the nitrate. Boron was added to the resulting gel as B_2O_3 or H_3BO_3 in stoichiometric amounts corresponding to $Al_{16}B_6Si_2O_{37}$ or $Al_8B_2Si_2O_{19}$, respectively, or in amounts in excess of these stoichiometries (Table 1; preliminary report in Pöter et al. 1998). Hydrothermal syntheses were carried out in 1996 and 1997 at 700–800 °C, 1–4 kbar (15–57 days duration) and 450–800 °C, 10 kbar (48–430 h duration); the stability of boralsilite was explored in a few runs at pressures to 30 kbar and temperatures to 1000 °C. Grains from runs B1, B3, B4, W1, and W4 were set in epoxy and mounted in plugs for EMPA.

Pöter et al. (1998) used an automated Siemens D500 powder diffractometer and a Philips PW1050 goniometer to examine run products ($5° < 2\theta < 65°$, Si standard). Several run products were re-examined (Table 1), at the Ruhr-Universität Bochum, using X-ray powder diffractograms recorded with a Siemens D5000 diffractometer and an image plate Guinier camera (G670 Huber). The D5000 diffractometer has a modified Debye-Scherrer geometry with the samples enclosed in 0.5 mm glass capillaries. Cu*K*α_1 radiation was obtained from a focusing Ge(111) monochromator. A position sensitive detector with an entrance window of 50 mm was used.

For the Rietveld refinement of the boralsilite structure, $^{VI}Al_8{}^{V}Al_8O_{10}(BO_3)_4(BO_4)_2(Si_2O_7)$, six scans were measured in the range from 10 to 100 °2θ with a step size of 0.0078° and a counting rate of 4 s per step. The scans were summed up in order to obtain a single data set. The Guinier camera is also equipped with a Ge monochromator, providing Cu*K*α_1 radiation. The 2θ range was 10 to 100° with a step size of 0.005°. Exposure time was 1 day. The crystal structure of boralsilite was refined according to the Rietveld method (Rietveld 1969) using the Jana2000 program package (Petříček and Dušek 2000; Dušek et al. 2001). Lattice parameters, four peak-shape parameters of the pseudo-Voigt profile function, and one parameter for a zero-point correction were refined. A Legendre polynomial with 22 parameters was used for the description of the background. The reflections are slightly broadened. The structure was initially refined with the atomic coordinates and the ideal formula $Al_{16}B_6Si_2O_{37}$ of natural boralsilite (Peacor et al. 1999). Common isotropic thermal displacement parameters were refined for all O atoms and for the cations in tetrahedral and threefold coordination. The interatomic distances, tetrahedral angles and O-B-O angles in the BO_3 units were restrained to remain close to the values of Peacor et al. (1999). A difference-Fourier analysis showed excess electron density at the Si, O10A, and O4 positions. The site-occupancy factors were refined in such a way that combined occupancies of the tetrahedral Si and B2 sites by B and Si (or Al) and vacancies on the O10A and O4 sites were allowed; this refinement yielded a significant reduction of the *R* values (from $R_{wp} = 4.70$ to 4.36) indicating mixed occupancy at the Si and B2 sites as well as incomplete occupancy of the O10A and O4 sites. A new difference-Fourier synthesis showed no residual electron density larger than 0.3 e^-, i.e., it gave no clear indication of electron density at the interstitial O10B site. In the final stages of the refinements, all atomic, profile, and background parameters were refined simultaneously. Corrections for absorption and extinction were found to be unnecessary. Preferred orientation was not observed. A Berar correction for serial correlations was carried out by multiplying the standard uncertainties with an appropriate factor (4.3) provided by the Jana2000 program to obtain statistically more realistic values (cf. Hill and Flack 1987). The quality of the refinement is only moderate, i.e., the goodness of fit is 2.44, but the Bragg *R* values are small enough that there should be no serious errors in the occupancies.

SYNTHETIC BORALSILITE AND "BORON-MULLITE"

Werding and Schreyer (1984) were the first to report the hydrothermal synthesis of a phase giving an X-ray diffraction (XRD) pattern similar to the orthorhombic phase $Al_{18}B_4O_{33}$ that Scholze (1956) synthesized at 1100 °C and 1 bar in the anhydrous Al_2O_3-B_2O_3 system and reported to have cell parameters close to those of mullite, but with two of them doubled. A similar "boron-mullite" was found as a breakdown product of alkali-free tourmaline at 600–850 °C, 2–8 kbar (e.g., Fig. 3) in the MgO-Al_2O_3-B_2O_3-SiO_2-H_2O system (Werding and Schreyer 1984) and dumortierite in the Al_2O_3-B_2O_3-SiO_2-H_2O system (Werding and Schreyer 1996). "Boron-mullite" could also be synthesized in the latter system at 800–1050 °C, 1 bar–4 kbar (Werding and Schreyer 1992; Pöter et al. 1998); in one case, the phase was reported to be $Al_8B_2Si_2O_{19}$ (Fig. 1). In addition to orthorhombic "boron-mullite," Pöter et al. (1998) succeeded in synthesizing a monoclinic phase identical to natural boralsilite and suggested that the previously synthesized samples of "boron-mullite" are metastable precursor phases to boralsilite.

XRD PROPERTIES AND CHEMICAL COMPOSITION OF ORDERED BORALSILITE

Using newer XRD instrumentation, we re-examined 14 of the 1997 experimental products reported by Pöter et al. (1998) and found that only four are ordered boralsilite (Table 1, Fig. 4a). Ordered boralsilite forms individual prismatic crystals up to 50 µm long and 20 µm wide partly encrusted with very fine prisms (e.g., Figs. 5a and 5b) or aggregates of finer prisms. The powder XRD pattern shows numerous sharp reflections characteristic of the pattern for ideal boralsilite and cell parameters could be calculated (Table 2). A fifth sample (B25) is better ordered than the disordered boralsilite described below, and could be almost as ordered as the four listed in Table 1, but critical peaks are obscured by the reflections from dumortierite and the OH-analogue of jeremejevite.

Electron-microprobe analyses of two relatively coarse-grained samples of ordered boralsilite (B1; W2) show that it contains less Si than natural boralsilite and that Al varies inversely with Si at constant B (Table 3, Fig. 6a). A Rietveld refinement of a sample

TABLE 1. Representative results of the 1996–1997 experimental studies, including all re-examined run products

Run	*T* (°C)	*P* (kbar)	Duration	Starting material*	Products*/Comments
Synthesis of boralsilite and "boron-mullite"					
B1	800	1	28 days	8:1 Gel + 50% H_3BO_3	Ordered Bor† (Fig. 5b) + amorph ϕ
B2	700	4	28 days	8:1 Gel + 50% H_3BO_3	Disordered Bor† (small amounts) + amorph ϕ + Qtz
B3	750	2	28 days	8:1 Gel + 50% H_3BO_3	Disordered Bor† (Figs. 5c–5d) + Qtz‡
B4	1050	1 bar	28 days	8:1 Gel + excess B_2O_3	B-Mul
B7	750	2	15 days	8:1 Gel + stoich H_3BO_3 + seed from B1	Disordered Bor†
B9	750	2	28 days	8:1 Gel + 50% H_3BO_3	Ordered Bor† + amorph ϕ
B13	700	10	48 h	8:1 Gel + 50% H_3BO_3	Bor + amorph ϕ
B14	800	10	74 h	B 13 prod (unwashed)	Bor + amorph ϕ
B23	700	10	172 h	γ – Al_2O_3 + 50% SiO_2 + 50% H_3BO_3	Bor + Dum(?)
B24	700	10	93 h	8:1 Gel + 10% H_3BO_3	Bor + no id
B25	450	10	430 h	8:1 Gel + 10% H_3BO_3	Ordered(?) Bor† + Jer + Dum
B26	800	1	57 days	8:1 Gel + 50% H_3BO_3	B-Mul† + disordered Bor† (Fig. 4b)
B27	800	1	57 days	8:1 Gel + 25% H_3BO_3	Ordered Bor† + amorph ϕ
B28	800	1	57 days	8:1 Gel + 10% H_3BO_3	Disordered Bor†
B29	800	1	57 days	8:1 Gel + stoich. H_3BO_3	Disordered Bor† (Fig. 4c)
B31	750	2	55 days	8:1 Gel + 50% H_3BO_3	B-Mul(?) + Bor
B33	750	2	55 days	γ-Al_2O_3 + SiO_2 + 50%‖ H_3BO_3	B-Mul(?)† + Disordered Bor† + Qtz
W2	700	4	28 days	4:1 Gel + 50% H_3BO_3	Ordered Bor† (Figs. 4a and 5a) + amorph ϕ
W4	1050	1 bar	28 days	4:1 Gel + excess B_2O_3	B-Mul
W6	750	2	28 days	4:1 Gel + stoich H_3BO_3	B-Mul† (Fig. 4d) + disordered Bor† (trace)+ Qtz
W7	750	2	28 days	4:1 Gel + 50% H_3BO_3	B-Mul† + disordered Bor† + Qtz
–§	830§	4§	240 h§	4:1 Gel + 100% H_3BO_3§	B-Mul containing 11.54 wt% B_2O_3; grain size <1 μm§
Breakdown of boralsilite					
B15	1000	10	70 h	B13 prod (unwashed)	Crn + no id
B18	700	20	96 h	B9 prod (washed) + H_2O (10 mg/2 mg)	Al_3BO_6 + Crn + Dum(?) cf. B21
B20	700	30	91 h	B9 prod (washed) + H_2O (10 mg/2 mg)	Crn + Al_3BO_6 + Dum(?)
B21	700	20	54 h	B9 prod (washed)	Bor + Al_3BO_6(?) + Dum(?) + B_2O_3(?). Bor disappeared in a longer run at this *P-T* condition (B18).

Notes: Abbreviations: amorph ϕ = a phase yielding no X-ray pattern; B-Mul = "Boron-mullite," in some cases resembling $Al_{18}B_4O_{33}$; Bor = boralsilite; Crn = corundum; Dum = dumortierite; Jer = OH analogue of jeremejevite; no id = no identification possible from the X-ray diffraction pattern; prod = products of another experiment; Qtz = quartz.

* Excess of H_3BO_3 or SiO_2 over the stoichiometric amount is given in percent. Products include H_3BO_3 in most cases.

† Run products re-examined with a Siemens D5000 diffractometer and an image plate Guinier camera (G670 Huber).

‡ Also found by EMPA of run product.

§ From Werding and Schreyer (1992).

‖ We suspect that less than 50% H_3BO_3 was actually weighed in the starting material.

of ordered boralsilite gave a structure (Table 4; Appendix Table 1[1]) similar to that of natural boralsilite from the Larsemann Hills (Peacor et al. 1999). Significant differences are substitutions at two cation sites (Si, B2) and vacancies at the O4 site, as well as at the O10A site. Substituting B for Si at the Si site and Al (not Si) for B at the B2 site is consistent with the EMPA results, i.e., these individual substitutions sum to Al substitution for Si (Fig. 6a). Partial occupancy at O4 could be related to incorporation of B at Si, but the resulting decrease in negative charge is not offset by the decrease of positive charge. The overall charge also is not balanced: +73.72 vs. –72.16. This discrepancy could be due either to undetected Al substitution for Si at the Si site, cation vacancies or to overlooked O. Detecting Al substitution for Si is difficult because the number of electrons is the same for Si^{4+} and Al^{3+}, and discernable lengthening of T-O bonds requires a relatively large amount of Al substitution. In boralsilite, the effects of simultaneous B substitution would offset any lengthening of the T-O bond. In addition, soft constraints were set for the interatomic distances to obtain regular tetrahedra. We tested for vacancies at the Al sites. The site-occupancy factors of some of the Al atoms were found to refine to lower values, but the deviations did not significantly exceed 1σ. There is no residual electron density larger than 0.38 e^-; these peaks are normal noise within the margin of error, and thus too low to be assigned to interstitial O. Peacor et al. (1999) reported occupancy at O10B in natural boralsilite, but the displacement parameter was found to be unusually large, suggesting that the O atom is not at a definite lattice position but smeared over a limited region. We doubt that O could have been found at O10B with Rietveld refinement. In summary, the lack of electron-density peaks shows that there is no charge at regular lattice sites, although this does not exclude the

TABLE 2. Cell parameters of synthetic boralsilite and "boron-mullite"

Run	*a* (Å)	*b* (Å)	*c* (Å)	β (°)	*V* (Å^3)
Ordered boralsilite (*C*2/*m*)					
W2	14.797(1)	5.5800(3)	15.095(2)	91.750(4)	1245.8(2)
B1	14.810(4)	5.5904(8)	15.105(4)	91.684(11)	1250.1(5)
B27	14.817(5)	5.5889(13)	15.114(5)	91.66(2)	1251.0(7)
Disordered boralsilite*					
B28	15.052(2)	5.5908(5)	15.237(3)	90.647(9)	1282.1(3)
B29	14.885(3)	5.6318(6)	15.119(2)	91.83(1)	1266.8(3)
B26	14.775(2)	5.6270(5)	15.124(2)	91.484(7)	1257.0(3)
B7	14.844(3)	5.6271(7)	15.075(3)	91.87(1)	1258.6(4)
W7	14.832(2)	5.6265(4)	15.050(2)	92.167(6)	1255.1(2)
"Boron-mullite"					
B26†	7.5197(8)	7.6685(7)	2.8403(3)	90	163.79(10)
W7†	7.4481(9)	7.6597(9)	2.8633(3)	90	163.56(8)
W6	7.505(1)	7.640(2)	2.8330(4)	90	162.44(6)
$Al_8B_2Si_2O_{19}$‡	7.513(9)	7.658(9)	2.841(4)	90	163.5(3)

* Indexed as being monoclinic like boralsilite (*C*2/*m*).

† Accompanies disordered boralsilite.

‡ Cell parameters calculated from Werding and Schreyer (1992) assuming a mullite unit cell and excluding the reflection at 20.301 °2θ.

[1] Deposit item AM-08-007, Appendix Tables 1–3. Deposit items are available two ways: For a paper copy contact the Business Office of the Mineralogical Society of America (see inside front cover of recent issue) for price information. For an electronic copy visit the MSA web site at http://www.minsocam.org, go to the American Mineralogist Contents, find the table of contents for the specific volume/issue wanted, and then click on the deposit link there.

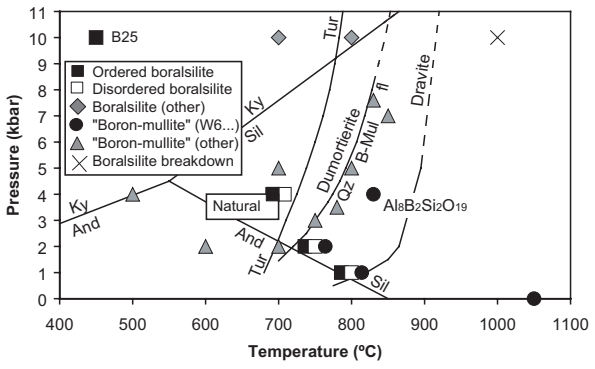

FIGURE 3. Pressure-temperature diagram summarizing syntheses of boralsilite and "boron-mullite" in Table 1. Filled squares = synthesis of ordered boralsilite, which includes B25 (Table 1). Open squares = synthesis of disordered boralsilite (Table 1). Gray diamonds = experimental products reported as boralsilite originally, but not re-examined to assess degree of order (only shown for 10 kbar runs). Filled circles = experimental products reported as "boron-mullite" in Table 1 and by Werding and Schreyer (1992, their $Al_8B_2Si_2O_{19}$) and Pöter et al. (1998); XRD pattern similar to the pattern for W6 (Fig. 4d). Gray triangles = experimental products reported as "boron-mullite" by Werding and Schreyer (1984, 1996) and Wodara and Schreyer (2001); no XRD pattern given (only shown if no overlap with later studies). X = breakdown of boralsilite for which degree of order was not re-examined. Superimposed symbols are separated for clarity. Box labeled "natural" indicates the *P-T* conditions estimated for natural boralsilite. Sources of other data: Al_2SiO_5 relations (Pattison 1992), dumortierite breakdown to quartz (Qtz) + "boron-mullite" (B-Mul) + fluid (fl) (Werding and Schreyer 1996), dravite breakdown (Robbins and Yoder 1962; Krosse 1995; Werding and Schreyer 1996), upper stability limit of schorl-dravite tourmaline (Tur) suggested for the Ryoke metamorphic belt, Japan (Kawakami 2004).

possibility of O atoms in defects. Thus, we have no explanation for the charge imbalance; a single-crystal structure study will be necessary to resolve the issue.

XRD PROPERTIES AND CHEMICAL COMPOSITION OF DISORDERED BORALSILITE AND "BORON-MULLITE"

The XRD patterns of seven run products differ from that of ordered boralsilite in that reflections are broadened and the intensity of the reflections is modified (Fig. 4c). In five cases, these products were originally considered to be "boron-mullite" similar to the compound $Al_8B_2Si_2O_{19}$ reported by Werding and Schreyer (1992). However, we believe that these run products more likely consist of disordered boralsilite because weak reflections of boralsilite can be found. Broadening could be due to either a very small size of coherently scattering domains or strain associated with lattice imperfections. The disordered boralsilite is neither microcrystalline boralsilite nor a mechanical mixture of boralsilite and an orthorhombic phase; testing the latter assumption did not give meaningful results for the lattice parameters. If we assumed that the products are disordered boralsilite, the lattice parameters (Table 2) could be refined with LeBail fits, but some anisotropic broadening had to be neglected. Simulations indicate that the intensity distribution cannot be explained by occupancy at O10B instead of at O10A.

Reflections of an orthorhombic phase in addition to those for boralsilite are definitely present in the XRD pattern of B26 and W7, which results in a set of doublets (e.g., Fig. 4b); the extra reflections could be indexed as mullite, as could those in the pattern for the single phase mixed with minor quartz in W6 (Fig. 4d). Cell volumes of these orthorhombic phases (Table 2) are 2–3% smaller than those of 3:2 mullite [e.g., 167.335(2) Å^3, Balzar and Ledbetter 1993] and 2:1 mullite [e.g., 168.04(3) Å^3, Angel and Prewitt 1986], most likely due to incorporation of

TABLE 3. Selected compositions of boralsilite

Type*	I	I	I	I	I	II	II	II	II	synthetic	synthetic
sample	905C I	121501E	121501E	121102B	121102B	112906B	112906B	HE138B2	HE138B2	B1	W2
note	holotype	dark BSE	light BSE	Fringe 1	Fringe 3	dark BSE	light BSE	dark BSE	light BSE		
no. analyses	12	8	9	13	18	9	9	7	7	9	4
wt%											
SiO_2	10.13	9.64	12.23	10.13	10.43	10.79	12.28	11.21	11.45	8.48	7.66
TiO_2	b.d	0.01	0.01	0.01	0.00	0.02	b.d.	0.02	0.01	0.02	0.03
Al_2O_3	70.41	71.42	70.50	70.37	70.77	68.94	67.73	70.80	68.65	72.71	73.43
FeO	0.54	0.29	0.34	1.02	0.71	1.87	2.28	0.80	1.72	0.16	0.10
MnO	b.d	b.d.	b.d.	b.d.	b.d.	b.d.	b.d.	0.01	0.01	b.d.	b.d.
MgO	0.003	b.d.	0.003	0.21	0.09	0.42	0.63	0.11	0.30	0.03	0.02
CaO	b.d.	0.005	0.01	0.02	0.03	0.04	0.01	0.01	b.d.	0.01	b.d.
BeO†	0.003	n.a.	n.a.	n.a.	n.a.	n.a.	n.a.	0.25	0.25	n.a.	n.a.
B_2O_3	18.69	17.85	16.42	17.55	17.30	17.71	16.92	16.60	16.55	17.77	17.89
As_2O_3	b.d.	b.d.	b.d.	n.a.	n.a.	b.d.	b.d.	b.d.	b.d.	b.d.	b.d.
Sum	99.77	99.23	99.52	99.32	99.34	99.79	99.84	99.81	98.94	99.17	99.14
Formulae											
O	37	37	37	37	37	37	37	37	37	37	37
Si	1.935	1.858	2.358	1.959	2.015	2.084	2.380	2.159	2.235	1.637	1.478
Ti	0.000	0.002	0.002	0.002	0.001	0.003	0.000	0.003	0.001	0.003	0.005
Al	15.860	16.217	16.018	16.039	16.112	15.694	15.468	16.077	15.787	16.537	16.711
Fe	0.086	0.047	0.055	0.166	0.114	0.302	0.369	0.128	0.281	0.026	0.017
Mn	0.000	0.000	0.000	0.000	0.001	0.000	0.000	0.002	0.002	0.000	0.000
Mg	0.001	0.000	0.001	0.061	0.027	0.121	0.182	0.032	0.087	0.009	0.005
Ca	0.000	0.001	0.001	0.004	0.006	0.008	0.001	0.003	0.000	0.001	0.000
Be	0.001	–	–	–	–	–	–	0.116	0.117	–	–
B	6.167	5.937	5.465	5.859	5.770	5.903	5.657	5.520	5.573	5.919	5.963
Sum	24.051	24.063	23.899	24.090	24.044	24.115	24.057	24.040	24.084	24.132	24.180
X_{Fe}	0.990	0.995	0.982	0.732	0.811	0.714	0.670	0.798	0.764	0.750	0.760

Notes: All Fe as FeO. X_{Fe} = Fe/(Fe + Mg). Dark/light BSE = appearance in back-scattered electron image. b.d. = below detection. n.a. = not analyzed.
* Compositional type.
† Ion microprobe analysis from Grew et al. (1998a).

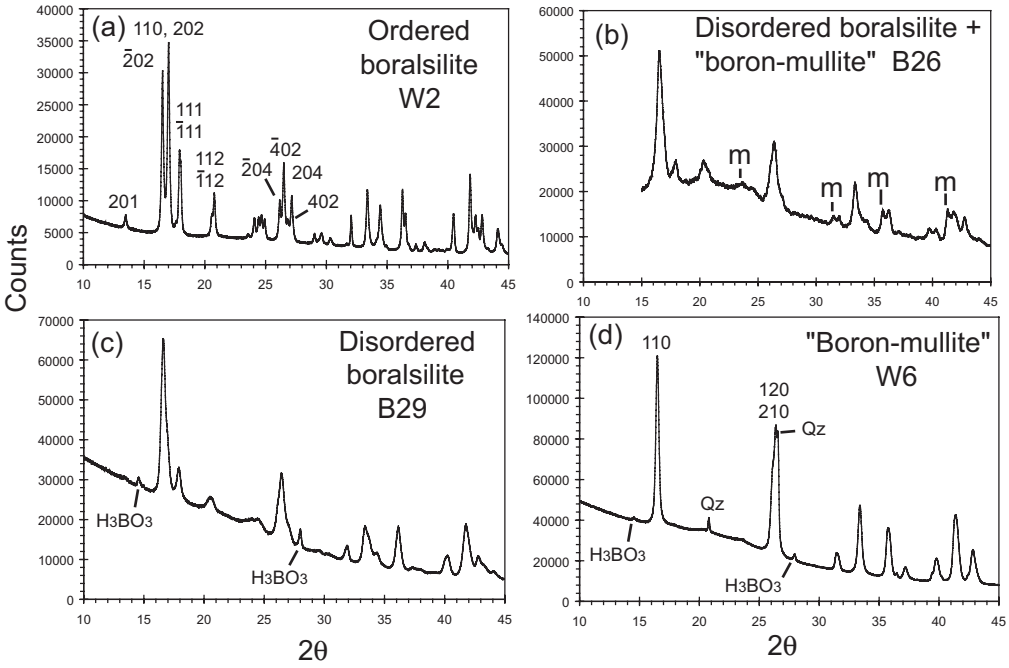

FIGURE 4. XRD patterns of experimental products. (**a**) Ordered boralsilite with a few reflections indexed. (**b**) Disordered boralsilite and "boron-mullite." m = reflections of "boron-mullite" not overlapping with boralsilite reflections. (**c**) Disordered boralsilite with minor H_3BO_3 impurity. (**d**) "Boron-mullite" with a few reflections indexed, minor quartz and H_3BO_3 impurities. The 101 quartz reflection is a shoulder on the 210 "boron-mullite" reflection.

TABLE 4. Summary of the Rietveld refinement of boralsilite in run W2

Site	constituent	occupancy natural*	occupancy synthetic	*x*	*y*	*z*	U_{iso}
Al1	Al	1	1	0.868(1)	0	0.343(1)	0.030(5)
Al2	Al	1	1	0.814(1)	0	0.160(1)	0.024(6)
Al3	Al	1	1	0.574(1)	0	0.074(1)	0.021(6)
Al4	Al	1	1	0.676(1)	0	0.339(1)	0.012(5)
Al5	Al	1	1	0.004(1)	0.255(2)	0.246(1)	0.019(3)
Al6	Al	1	1	0.75	0.25	0	0.017(7)
Al7	Al	1	1	0.75	0.25	0.5	0.010(7)
Si	Si	1	0.86(4)†	0.424(1)	0	0.419(1)	0.007(6)
Si	B	0	0.14(4)†	0.424(1)	0	0.419(1)	0.007(6)
B1	B	1	1	0.096(1)	0	0.098(1)	0.007(6)
B2	B	1	0.88(4)†	0.379(1)	0	0.118(1)	0.007(6)
B2	Si/Al	0	0.12(2)†	0.379(1)	0	0.118(1)	0.007(6)
B3	B	1	1	0.138(2)	0	0.360(2)	0.007(6)
O1	O	1	1	0.764(2)	0	0.269(2)	0.010(2)
O2	O	1	1	0.798(2)	0	0.440(2)	0.010(2)
O3	O	1	1	0.919(2)	0	0.218(2)	0.010(2)
O4	O	1	0.91(2)	0.936(1)	0.739(3)	0.357(1)	0.010(2)
O5	O	1	1	0	0.5	0.5	0.010(2)
O6	O	1	1	0.325(2)	0	0.457(1)	0.010(2)
O7	O	1	1	0.322(1)	0.214(3)	0.106(1)	0.010(2)
O8	O	1	1	0.702(2)	0	0.074(2)	0.010(2)
O9	O	1	1	0.068(1)	0.214(1)	0.134(1)	0.010(2)
O10A	O	0.95	0.72(4)	0.452(2)	0.0000	0.048(2)	0.010(2)
O10B	O	0.0726	0	0	0.5	0	0.010(2)
O11	O	1	1	0.166(1)	0.214(1)	0.397(1)	0.010(2)
O12	O	1	1	0.578(2)	0	0.280(2)	0.010(2)
O13	O	1	1	0.421(1)	0	0.204(2)	0.010(2)
O14	O	1	1	0.069(2)	0	0.296(2)	0.010(2)
O15	O	1	1	0.167(1)	0	0.041(2)	0.010(2)

Note: R_p = 3.18, R_{wp} = 4.36, R_{obs}(Bragg) = 2.85, Rw_{obs}(Bragg) = 2.80.
* From Peacor et al. (1999).
† Restrained to full occupation of the Si and B2 sites.

B (see below). A very broad, low hump between 20.0 and 20.4 °2θ in W6 is close to the peak at 20.3 or 20.5 °2θ in the patterns for disordered boralsilite, itself corresponding to the $\bar{1}12$ and 112 reflections in ordered boralsilite, and thus could be due to incipient development of a boralsilite-like structure. The patterns reported for $Al_8B_2Si_2O_{19}$ (Werding and Schreyer 1992) and for

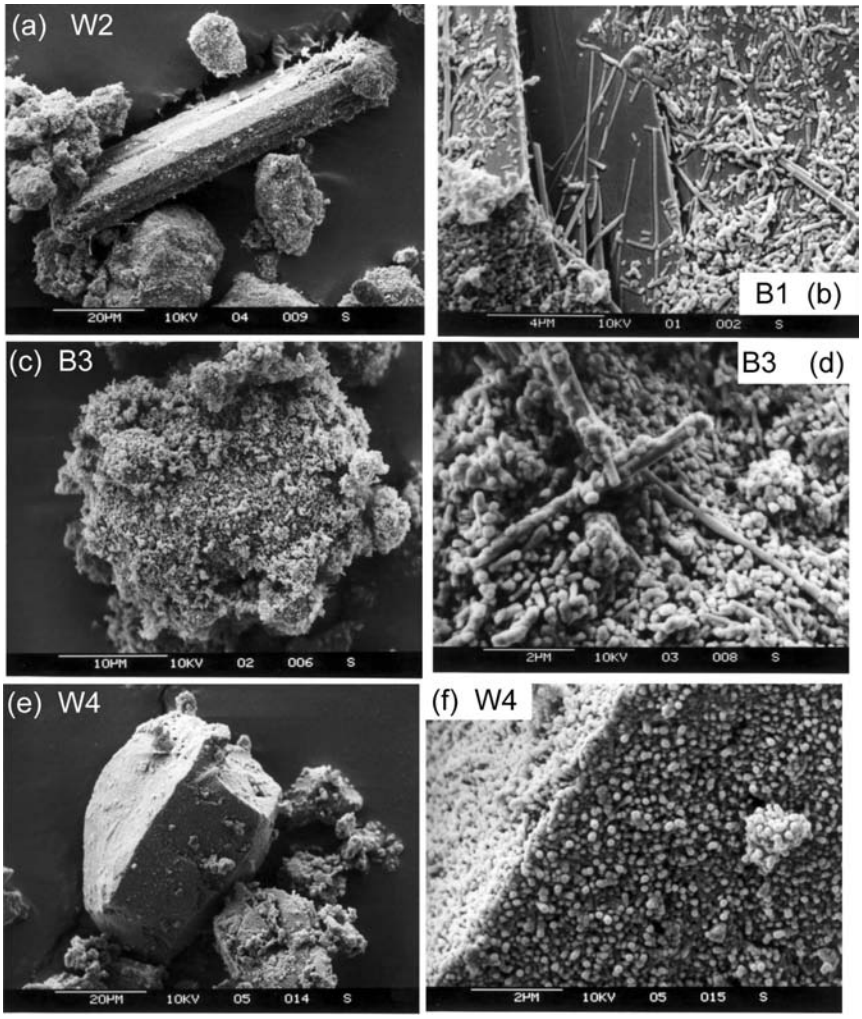

Figure 5. Images obtained by scanning electron microscopy of run products. (**a**) Prism of ordered boralsilite among grains of the amorphous phase. (**b**) Very fine-grained prisms on the surface of a prism of ordered boralsilite. (**c**) An aggregate of disordered boralsilite. (**d**) A close-up of an aggregate of disordered boralsilite. (**e**) Aggregate of "boron-mullite." (**f**) Same aggregate as **e** but magnified.

syntheses at 1050 °C and 1 bar (B4 and W4; Table 1) are similar to Figure 4d except that this reflection, which is found at 20.301, 20.433, and 20.395 °2θ, respectively, is more prominent, i.e., the development of boralsilite apparently has proceeded further. The presence of this single reflection made it necessary for Werding and Schreyer (1992) to index its powder XRD pattern with a supercell having two doubled cell parameters; we indexed its powder XRD pattern with a mullite cell to give cell parameters very similar to those for "boron-mullite" W6 (Table 2).

SEM images of the run product of B3 show irregular masses with a knobby surface (Fig. 5c) in places with fine prisms (Fig. 5d); we presume that these masses are aggregates of disordered boralsilite. In contrast, grains of "boron-mullite" in W4 show discrete edges and relatively smooth, quasi-planar faces (Figs. 5e and 5f), but these grains also seem to be highly porous aggregates. The grain of analyzed disordered boralsilite in epoxy plug B3 has an irregular outline, whereas the analyzed "boron-mullite" grains in epoxy plugs B4 and W4 have a polygonal outline; i.e., the analyzed grains in the plug mount appear to be the same material as the grains imaged with the SEM. Compositions of disordered boralsilite plot in a roughly linear trend passing about midway between $Al_8B_2Si_2O_{19}$ and $Al_{16}B_6Si_2O_{37}$, i.e., disordered boralsilite differs in composition from ordered boralsilite (Fig. 7). "Boron-mullite" compositions plot a relatively tight trend between $Al_8B_2Si_2O_{19}$ and the Al borate $Al_{18}B_4O_{33}$, with the material synthesized from the 4:1 gel (W4) being more siliceous than material synthesized from the 8:1 gel (B4). This result is consistent with the inference of Werding and Schreyer (1992) that the composition of their "boron-mullite" is $Al_8B_2Si_2O_{19}$, because they obtained a single-phase product from the 4:1 gel composition and a B content (11.54 wt% B_2O_3) consistent with this formula. The composition of the "boron-mullite" synthesized from a 3:1 gel + melted B_2O_3 by Letort (1952) plots along this trend, but at higher Al_2O_3/SiO_2 ratio despite the lower Al_2O_3/SiO_2 ratio of the starting gel. The distinct trends for disordered boralsilite and "boron-mullite," together with simultaneous presence of both in some run products, e.g., B26, W7 (Table 1, Fig. 4b), suggests the absence of a gradation between the two phases.

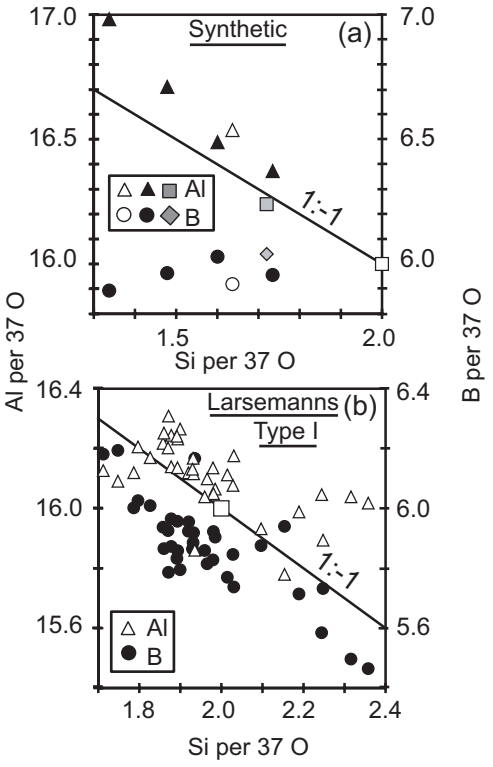

Figure 6. (**a**) Compositions of synthetic boralsilite from runs B1 (ordered, filled symbols) and W2 (ordered, unfilled symbols). Gray-filled symbols represent the composition of W2 refined by the Rietveld method (assuming that only Al replaces B at the B2 site). (**b**) Compositions of boralsilite in samples 121502E, 020602A, 121102B, 121102C, and holotype (8812905-1 and -2) from the Larsemann Hills (Type I). Open squares indicate ideal composition $Al_{16}B_6Si_2O_{37}$. The lines indicate the ideal substitutions.

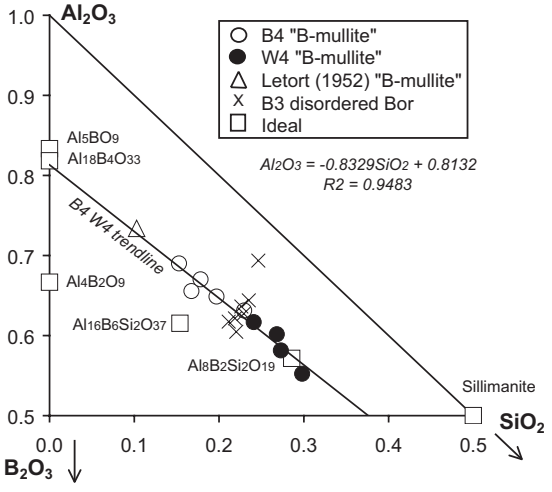

Figure 7. Compositions of "boron-mullite" synthesized from gels at 1050 °C and 1 bar (B4, W4, this study) and at 930 °C and 1 bar (3:1 gel, Letort 1952) plus compositions of disordered boralsilite (B3) in mol% oxide. Trend line is based on least-squares fit to the nine points for "boron-mullite" B4 and W4.

The "amorphous" phase

SEM images of the run product of B1 and W2 showed that ordered boralsilite is associated with irregular knobby masses (e.g., Fig. 5a), which we presume is amorphous because it did not give an XRD pattern. Similar appearing material in the plugs for B1 and W2 is extremely heterogeneous; energy-dispersive and wavelength-dispersive scans revealed that Al is far more abundant than Si and that substantial B is present, that is, the composition is similar to disordered boralsilite and "boron-mullite."

Formation conditions of synthetic boralsilite and "boron-mullite"

Boralsilite and "boron-mullite" have been synthesized hydrothermally in the B_2O_3-Al_2O_3-SiO_2-H_2O (±MgO) system over a wide range of temperatures at pressures up to 10 kbar (Fig. 3). Boralsilite (ordered and disordered) was found in syntheses between 450 and 800 °C. The only synthesis below 700 °C, i.e., B25 at 450 °C and 10 kbar, also yielded substantial amounts of dumortierite and the OH-analogue of jeremejevite, which have been synthesized at similar temperatures in other experiments (Stachowiak and Schreyer 1998; Wodara and Schreyer 2001). Boralsilite has broken down by 1000 °C (Fig. 3) and at 20 kbar (Table 1). It is likely that disordered boralsilite is metastable, whereas ordered boralsilite could be stable at 700–800 °C, 1–4 kbar, as Pöter et al. (1998) suggested. Nonetheless, it remains unclear what physical-chemical conditions favor transformation of disordered to ordered boralsilite. It involves a change of composition, at least in some cases (Figs. 1 and 7). There is no evidence that duration, gel composition, or proportion of H_3BO_3 played a critical role. One run (B7) was seeded with ordered boralsilite from B1, but this did lead to the formation of ordered boralsilite. Of the 14 run products that were re-examined, five contained an apparently amorphous phase and four of these yielded ordered boralsilite. This observation suggests that another factor could play a role, for example, the chance seeding by an unknown impurity in some runs resulted in a portion of the material crystallizing to ordered boralsilite that coarsened rapidly amid a residue that failed to crystallize sufficiently to give reflections in an XRD pattern, even in runs as long as 57 days (run B27; Table 1).

A natural "boron-mullite"?

A mineral provisionally identified as "boron-mullite" has been found in three specimens of SiO_2-undersaturated, B-rich metapelites from Mount Stafford, central Australia. Specimens MSTgran and 95-175D originate from a stratiform grandidierite-bearing lens in metapelitic migmatite and cordierite granofels in metamorphic zone 4 (granulite facies), close to the boundary with zone 3 (transitional between the upper amphibolite facies and the lower granulite facies). Specimen MST1002 was found in float within zone 4 (Buick et al. 2006 and unpublished manuscript).

All three specimens are dominated by cordierite, hercynite, and K-feldspar (Buick et al. 2006 and in preparation). Biotite and andalusite porphyroblasts are also major constituents in MST1002, but the andalusite is replaced by sillimanite aggregates in the other two specimens. Small amounts of relict tourmaline

are present in MST1002. Relatively coarse prisms of grandidierite are characteristic of MSTgran and 95-175D, whereas in MST1002, grandidierite enclosing abundant fine ilmenite is found only as an overgrowth on werdingite. Prisms of werdingite (X_{Fe} = 0.49–0.62, e.g., MST1002, Table 5) most typically form a fringe on andalusite or sillimanite bundles replacing it; there also are loose aggregates of subparallel prisms in cordierite.

"Boron-mullite" is visible only in back-scattered electron images (Fig. 8). This identification is based solely on chemical composition (see below); we have no XRD data to confirm that the analyzed phase is related to mullite. The mineral occurs exclusively as a replacement of werdingite, generally in the vicinity of andalusite or sillimanite, which it could also be replacing; it is also commonly in contact with cordierite, and locally with hercynite, biotite, and K-feldspar (as an inclusion). The "boron-mullite" is heterogeneous at a very fine scale; sections viewed roughly down the **c** axis appear as a patchwork of different shades of gray, whereas sections viewed at a high angle to it show banding (Figs. 8b, 8c, and 8d), in both cases due to compositional variation, and suggesting that "boron-mullite" is fibrous.

Attempts to analyze a given area of apparently homogeneous electron-scattering intensity with the electron microprobe failed to give consistent results, requiring us to treat each spot analysis individually (Fig. 9, Table 6) instead of averaging them. Its composition extends without break from nearly stoichiometric Al_2SiO_5 almost halfway across the BAS triangle toward the aluminoborate Al_5BO_9 (Fig. 1). A least-squares fit to the data gives SiO_2 16.5, Al_2O_3 76.2, B_2O_3 7.1, Sum 99.8 wt% as the end point of the compositional range. Although the range of compositions overlaps with those of the three samples of "boron-mullite" synthesized at high temperatures by Dietzel and Scholze (1955), the natural "boron-mullite" contains stoichiometric Al_2SiO_5 as one component, not $Al_6Si_2O_{13}$ (3:2 mullite) as inferred by investigators of the high-temperature phases. The trend for the Mount Stafford "boron-mullite" is also distinct from the trend for "boron-mullite" synthesized from gels (Fig. 1).

Metapelites, metapsammite, and metabasites from the Mount Stafford area experienced low-pressure/high-temperature metamorphism (e.g., Vernon et al. 1990; Greenfield et al. 1998; White et al. 2003), and zone 4 reached granulite-facies conditions (a minimum temperature of 775–785 °C at 3.3–4 kbar, White et al. 2003). Within this zone, metapsammites and moderate-Al metapelites commonly contain the assemblage quartz + biotite + cordierite + K-feldspar ± orthopyroxene ± garnet, and high-Al metapelites, quartz + K-feldspar + biotite + cordierite + sillimanite + hercynite (e.g., Greenfield et al. 1998; White et al. 2003). The formation of grandidierite, werdingite, and "boron-mullite" is closely tied to partial melting of B-rich metapelite during which tourmaline, relics of which remain in MST1002, is a reactant, and werdingite and grandidierite are products in samples 95-175D and MSTgran, and werdingite alone in MST1002, at close to peak temperatures (780 °C, 3.3–4 kbar for the boundary between zones 3 and 4, White et al. 2003). "Boron-mullite" could have resulted from either retrograde or prograde breakdown of werdingite. Werding and Schreyer (1992) reported the incongruent melting of werdingite to a "boron-mullite" at 1200 °C, 1 bar under nearly anhydrous conditions. Although this temperature far exceeds those estimated for Mount Stafford, we cannot rule out the possibility that at higher pressures in the presence of granitic melt, werdingite could have melted incongruently at much lower temperatures.

TABLE 5. Selected compositions of grandidierite (Gdd) and werdingite (Wrd)

Mineral	Gdd	Gdd	Wrd	Wrd	Wrd
sample	010205J4	121102B	121102B	HE138B2	MST1002
note		Fringe 1	Fringe 1	light BSE	
no. analyses	13	16	16	9	8
wt%					
SiO_2	19.72	19.88	18.86	18.66	19.52
TiO_2	0.01	b.d.	0.02	b.d.	0.02
Al_2O_3	50.21	50.28	61.36	60.89	62.05
FeO	8.16	8.14	4.05	7.11	6.40
MnO	0.02	0.07	0.02	0.04	0.01
MgO	9.69	9.30	3.67	1.61	2.33
CaO	b.d.	0.01	0.01	b.d.	b.d.
BeO*	n.a.	n.a.	n.a.	0.19	n.a.
B_2O_3	11.83	11.30	11.30	11.67	9.88
As_2O_3	b.d.	n.a.	n.a.	b.d.	b.d.
Sum	99.63	98.99	99.29	100.17	100.21
Formulae					
O	9	9	37	37	37
Si	0.985	1.002	3.785	3.751	3.943
Ti	0.000	0.000	0.002	0.000	0.003
Al	2.957	2.985	14.514	14.429	14.771
Fe	0.341	0.343	0.681	1.195	1.082
Mn	0.001	0.003	0.003	0.007	0.001
Mg	0.722	0.699	1.098	0.483	0.702
Ca	0.000	0.001	0.002	0.000	0.000
Be	–	–	–	0.092	–
B	1.020	0.983	3.914	4.051	3.445
Sum	6.026	6.015	23.999	24.009	23.946
X_{Fe}	0.321	0.329	0.383	0.712	0.606

Notes: All Fe as FeO. X_{Fe} = Fe/(Fe + Mg). Dark/light BSE = appearance in back-scattered electron image. b.d. = below detection. n.a. = not analyzed.
* Ion microprobe analysis from Grew et al. (1998b).

CURRENT STATUS OF "BORON-MULLITE"

Werding and Schreyer (1996) suggested that the ternary compositional range of "boron-mullite" occupies a quadrilateral with vertices at 2:1 mullite, 3:2 mullite, $AlBO_3$, and Al_5BO_9 (Fig. 1). However, solid solution between 3:2 mullite and $Al_{18}B_4O_{33}$ (dashed line in Fig. 1) and their own phase $Al_8B_2Si_2O_{19}$ (Werding and Schreyer 1992) constituted the only evidence at the time for ternary phases in the quadrilateral. No naturally occurring ternary phases were known until boralsilite was discovered.

The results of the present study suggest the presence of at least two solid-solution series extending into the "boron-mullite"

TABLE 6. Selected compositions of "boron-mullite" (B-Mul) and disordered boralsilite (dis Bor)

Mineral	B-Mul	B-Mul	dis Bor	B-Mul	B-Mul	B-Mul
sample	B4	W4	B3	MST1002	95-175D	MST1002
note				lowest Si	mid Si	high Si
Grain				4	4	2
no.	2	6	5	1	1	1
wt%						
SiO_2	9.83	11.18	10.68	16.49	23.85	35.20
TiO_2	b.d.	b.d.	b.d.	b.d.	0.01	0.03
Al_2O_3	54.88	48.59	49.74	76.45	71.64	64.24
FeO	0.14	0.11	0.13	0.62	0.37	0.41
MnO	b.d.	b.d.	0.01	0.01	0.01	0.02
MgO	0.03	0.02	0.03	0.20	0.06	0.08
CaO	0.03	0.01	0.02	b.d.	b.d.	b.d.
B_2O_3	8.91	7.65	9.83	5.73	4.46	0.20
As_2O_3	n.a.	n.a.	n.a.	b.d.	b.d.	b.d.
Sum	73.82	67.56	70.42	99.51	100.41	100.17

Note: All Fe as FeO.

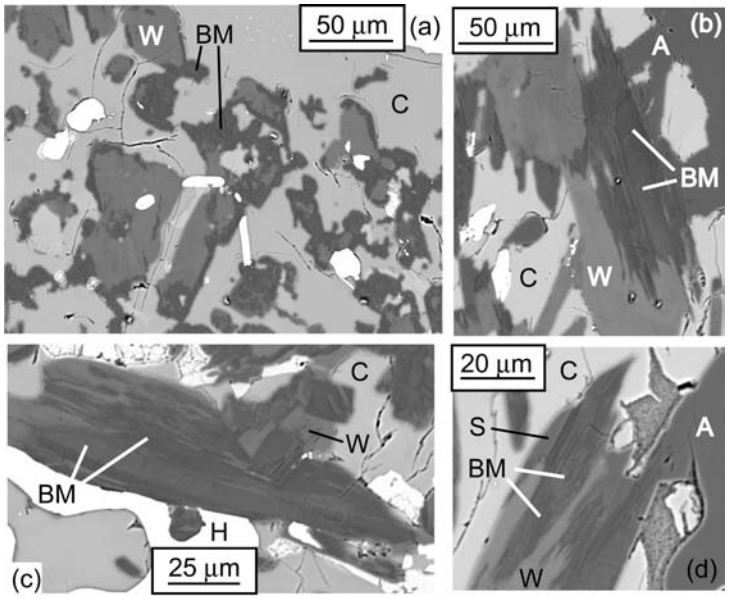

FIGURE 8. Back-scattered electron images of borosilicates in metapelites from Mount Stafford, central Australia. (**a**) "Boron-mullite" replacing werdingite in a cordierite matrix. Light grains are hercynite (subequant) and ilmenite (tabular). Sample 95-175D. (**b**) Banded "boron-mullite" has replaced werdingite adjacent to andalusite. Werdingite shows indistinct zoning. Sample MST1002. (**c**) Banded "boron-mullite" has replaced werdingite. Sample MSTgran. (**d**) Banded "boron-mullite" has replaced werdingite. Lightest bands (S) approach sillimanite in composition. Sample MST1002. Abbreviations: A = andalusite, BM = "boron-mullite", C = cordierite, H = hercynite, S = sillimanite-like, W = werdingite.

quadrilateral, one extending from sillimanite toward Al_5BO_9 in what is presumed to be a natural "boron-mullite," and the other from $Al_8B_2Si_2O_{19}$ toward $Al_{18}B_4O_{33}$ in material synthesized from gels. The three compositions of "boron-mullite" synthesized from melt plot close to the trend for the presumed natural "boron-mullite," raising the possibility that the synthetic solid solution proposed by Gielisse and Foster (1961) extends to sillimanite rather than to mullite.

Werding and Schreyer (1996) suspected that "boron-mullite" would be largely metastable over the proposed compositional range, a suspicion borne out by restriction of "boron-mullite" compositions to two narrow bands. Many of the hydrothermal syntheses of "boron-mullite" are within the stability field of dumortierite (Fig. 3) and could be metastable, especially in the presence of quartz. However, the compositions plotted in Figures 1 and 7 are those of "boron-mullite" synthesized at temperatures well above the stability of dumortierite. In addition, the rocks containing the presumed natural "boron-mullite" were affected by temperatures above the stability of dumortierite at <4 kbar. In summary, there is good reason to think that "boron-mullite" has a stability field at high temperatures and low pressures in rocks sufficiently rich in B.

Natural boralsilite

Boralsilite is a relatively widespread, albeit minor, constituent of pegmatites belonging to two generations in the Larsemann Hills, one associated with the D_2-D_3 deformation and the second with D_4 (deformation scheme of Carson et al. 1995). The earlier generation typically forms irregular pods or veins ranging from a few decimeters to a meter or so in thickness; larger bodies extend 100 m or more and are mapped as Rumdoodle pegmatite (Carson and Grew 2007; this paper, Fig. 10). The bodies are either roughly concordant or crosscut S_2 and S_3 fabrics; in places, they are folded and show an axial-planar fabric. The later generation consists of undeformed, generally planar, cross-cutting veins a few centimeters to a few decimeters in thickness. Characteristic of both generations of pegmatites are graphic tourmaline-quartz

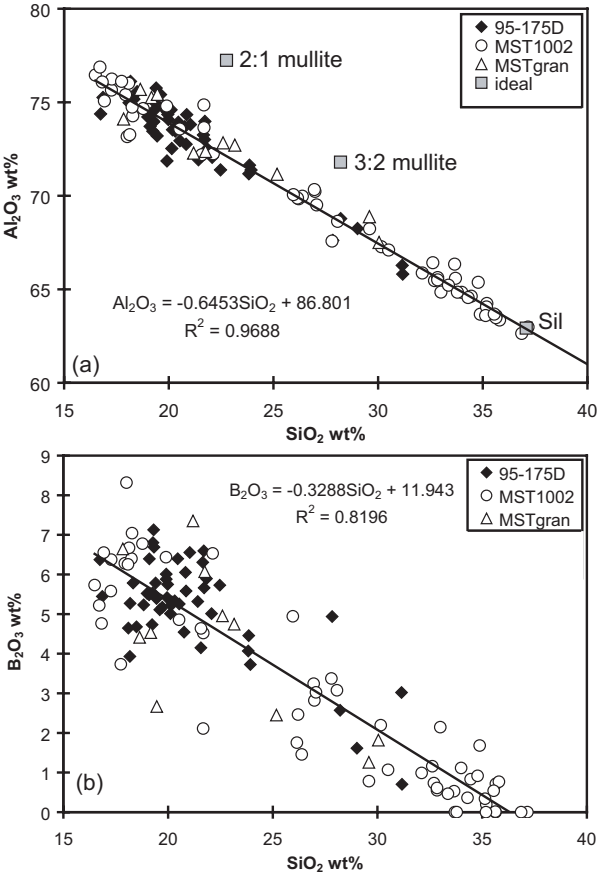

FIGURE 9. Compositions of "boron-mullite" in B-rich metapelitic rocks from Mount Stafford, central Australia. Plotted data are the results of individual analyses on three or four grains in each of the three sections; only analyses totaling 98–102 wt% and containing less than 0.5 wt% MgO and 1.2 wt% FeO, i.e., negligible werdingite impurity, are plotted. Ratios refer to Al_2O_3: SiO_2 (mol) in mullite. Sil = sillimanite. Lines are least-squares fits to the data.

intergrowths, commonly associated with bright red microcline (Fig. 11a), but also occurring in plagioclase (Figs. 12a and 12b). Seven of the nine pegmatites in which boralsilite has been identified belong to the D_2-D_3 generation and six intersect one of the four B-enriched units containing prismatine, grandidierite, and tourmaline; the other three pegmatites cut nearby units instead (Fig. 10). Pegmatites containing prismatine or grandidierite, but not boralsilite, are D_2-D_3 pegmatites also cutting the four B-enriched units. Early dumortierite is present only in D_4 pegmatite veins at locality 121502. In contrast, tourmaline, including graphic intergrowths with quartz, occurs in pegmatites further from the borosilicate-bearing metamorphic units, e.g., between the northern and southern areas of borosilicate-rich rocks on Stornes Peninsula shown in Figure 10.

Typically, boralsilite forms bundles and sprays of prisms, in places euhedral, in quartz or rarely K-feldspar, most commonly near the graphic tourmaline-quartz intergrowths (Grew et al. 1998a; this paper, Figs. 11c and 11d). Minerals closely associated with boralsilite (Appendix Table 2[1]) in the samples collected in 2003–2004 include plagioclase, from which it is commonly separated by quartz (Fig. 13b), primary dumortierite, grandidierite (e.g., Fig. 11e), werdingite, sillimanite (121102B only), and prismatine (121102C only, Figs. 12a and 12b). Primary dumortierite forms gray bundles of subparallel prisms up to 2 cm long; a few bundles exceed 1 cm in width. Grandidierite forms early, relatively coarse-grained prisms in a few cases (e.g., Fig. 11e), but in other it is a later phase (e.g., Figs. 12b and 12d). Werdingite is present in a single section from locality 121102 (Table 5), which is the sixth known locality worldwide (Grew et al. 1998b; Buick et al. 2006) and the first for Antarctica. Apatite is present in every boralsilite-bearing section (e.g., Fig. 12f); monazite, zircon, and rutile are less common. Grew et al. (1998a) reported boralsilite being replaced by foititic-olenitic tourmaline, diaspore, and kaolinite(?); other secondary minerals in the newly collected samples are andalusite (Fig. 11e) and bright-blue dumortierite, which is found in five of the nine pegmatites. Biotite, cordierite, and wagnerite are also present in boralsilite-bearing pegmatites, but not in close proximity to boralsilite.

Sections 121102B and 121102C offer particular insight into the sequence of crystallization of the borosilicates. Primary tour-

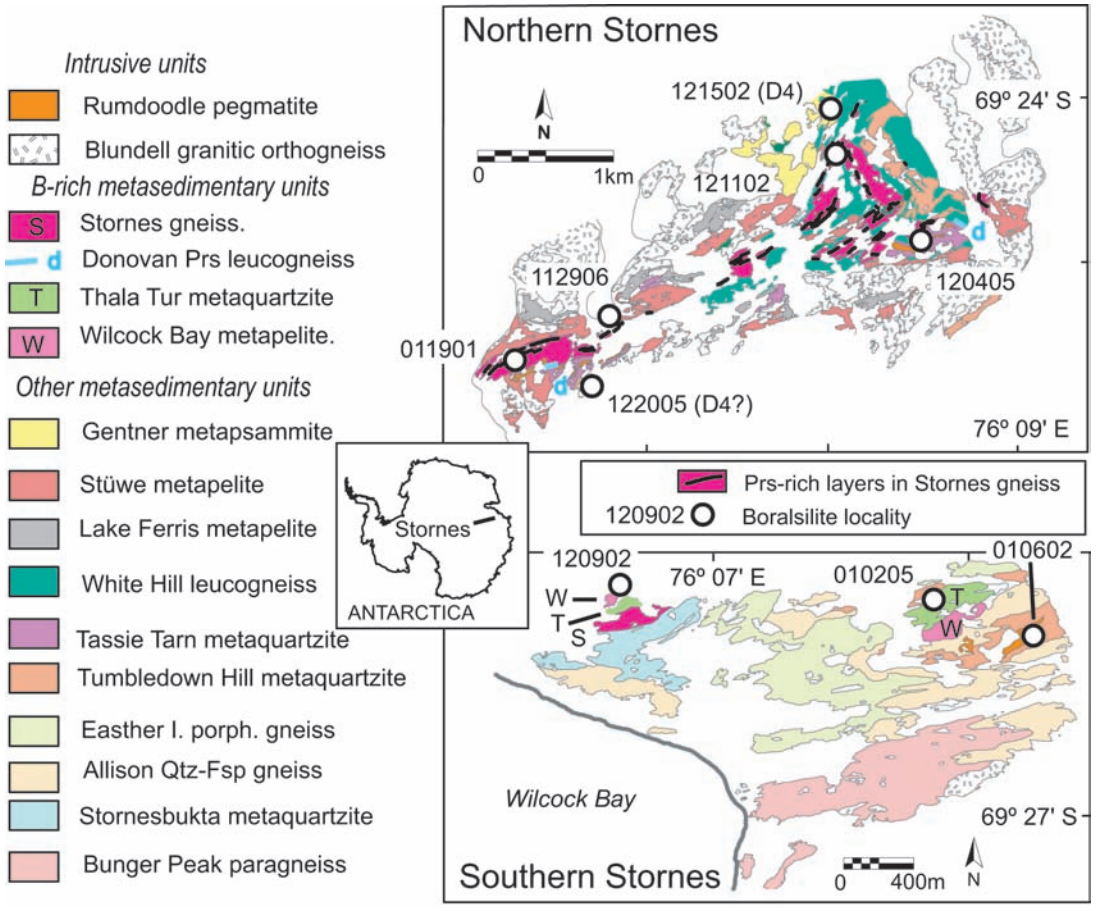

FIGURE 10. Geologic maps of B-rich metamorphic rocks in the Stornes Peninsula (modified from Carson and Grew 2007) showing localities for boralsilite collected during the 2003–2004 season (open circles; GPS coordinates are given in Appendix Table 3). The holotype sample was collected near locality 121102 (Douglas Thost, personal communication, 1991). Boralsilite was identified using optical microscopy or the electron microprobe except 122005. D_4 indicates the one locality where borasilite occurs in second-generation pegmatite veins; the veins at 122005 could also be D_4. Prs = prismatine; Tur = tourmaline, Qtz-Fsp = quartzofeldspathic. The order in which the metasedimentary units are listed does not correspond to relative depositional age, which remains indeterminate.

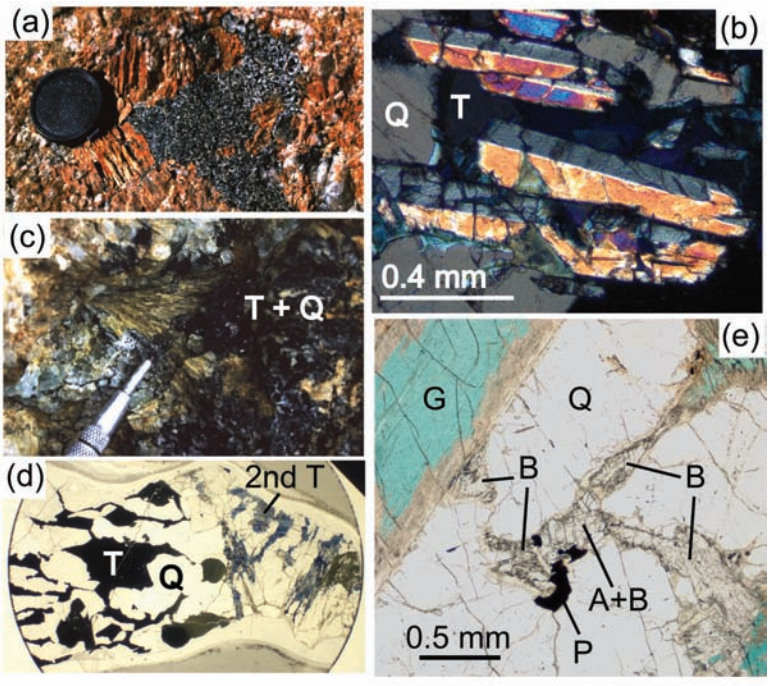

FIGURE 11. Photographs of mineral associations in pegmatites from the Larsemann Hills, East Antarctica. (**a**) Graphic tourmaline-quartz intergrowth (black and white) in coarse-grained red microcline, D_2-D_3 pegmatite at locality 113001, about 100 m SW of locality 112906. Lens cap is 5 cm in diameter. (**b**) Photomicrograph of twinned prisms of boralsilite overgrown by secondary tourmaline, which is at extinction. Cross-polarized light, sample 120902G. (**c**) Radiating fibrous bundle of boralsilite (stained yellow above pointer) adjacent to graphic tourmaline-quartz intergrowth in a D_2-D_3 pegmatite at locality 121102. (**d**) Photomicrograph of acicular, partially altered boralsilite adjacent to a graphic tourmaline-quartz intergrowth. Boralsilite is largely engulfed in olive and blue secondary tourmaline. Diameter of section is 2.5 cm. Plane polarized light, sample 120405D. (**e**) Photomicrograph of aggregates of boralsilite in quartz near grandidierite. Secondary andalusite encloses boralsilite (A+B). Pyrite is partially replaced by oxide. Plane-polarized light, sample 112906B. Abbreviations: A = andalusite, B = boralsilite, G = grandidierite, P = pyrite, Q = quartz, T = tourmaline.

maline is limited to the graphic tourmaline-quartz intergrowths (Figs. 12a and 12b), in some of which coarse-grained biotite is also found. Prismatine in prisms up to 1 cm in length is present in coarse-grained plagioclase surrounding the graphic tourmaline-quartz intergrowths in 121102C; terminations of the prisms appear to have been embayed, suggesting the prisms might be xenocrysts. Boralsilite is present with quartz in the plagioclase, whereas a few fine grains of grandidierite occur around the prismatine (e.g., Fig. 12b) or in plagioclase. Grandidierite is also later than prismatine in the pegmatite at locality 010205, but in this case, grandidierite is relatively coarse-grained and appears to be a relatively early phase. In section 121102B, grandidierite (Table 5), werdingite, and boralsilite form fringes on aggregates of sillimanite prisms (Figs. 12c–12f). Boralsilite also coarsens away from the aggregates to form independent prisms, e.g., the prism to the left in Figure 12e. In summary, tourmaline in graphic intergrowth with quartz, rare dumortierite, and some grandidierite crystallized early in the Larsemann Hills pegmatites, whereas boralsilite, rare werdingite, and most grandidierite crystallized later, followed by a second generation of tourmaline and dumortierite. Prismatine is an early phase, but we cannot exclude the possibility that it is xenocrystic in the pegmatites, having been plucked from segregations in the source rocks.

In terms of composition, there are two types of boralsilite in the Larsemann Hills pegmatites (Table 3). Type 1, including the holotype specimen, is the more common; prisms are heterogeneous (Figs. 13a and 13c). Electron scattering increases with Si, which varies inversely with B over a narrow range of Si (Fig. 6b). Variation of Al is roughly inverse with Si for Si < 2 atoms per 37 O, but is nearly independent of Si for Si > 2 atoms per 37 O, consistent with very limited solid solution toward sillimanite (Fig. 1).

Type-II boralsilite has been found in two samples (112906, 010205, Fig. 14a) also containing grandidierite (e.g., Fig. 11e); it also appears heterogeneous in BSE images. Variations of Si, (Fe + Mg), Al and B are consistent with a solid solution of up to 30% of an ideal werdingite component, $(Fe,Mg)_2Al_{14}B_4Si_4O_{37}$, in boralsilite (Fig. 14a). Boralsilite associated with werdingite and grandidierite in sample 121102B is Type I, but with higher MgO and FeO than other Type I (Table 3).

Boralsilite from Almgjotheii, SW Norway, the only other known locality of the mineral (Grew et al. 1998a), was also re-analyzed using the method described above (e.g., Table 3). Boron decreases with Si, but an increase of (Fe + Mg + Mn) with Si is less evident than in type II from the Larsemann Hills; the maximum werdingite content is also 30% (Fig. 14b). Like type II, the Almgjotheii boralsilite is associated with grandidierite, but differs in being intergrown with werdingite (e.g., Table 5) in a texture suggesting exsolution and not found in the werdingite-boralsilite fringes in the Larsemann Hills (e.g., Fig. 12f).

The boralsilite-bearing pegmatites in the Larsemann Hills and at Almgjotheii differ from most tourmaline-bearing pegmatites in being associated with granulite-facies rocks. We interpret the Larsemann Hills pegmatites to be derived by anatexis of B-rich metamorphic rocks containing prismatine, grandidierite, and tourmaline under granulite-facies conditions. Conditions for boralsilite formation in the Larsemann Hills were originally estimated to be 750 °C, 4–5 kbar, that is, near the conclusion of decompression following peak conditions. The presence of andalusite-bearing melts in the southern Stornes Peninsula suggests that some melting occurred close to the andalusite-sillimanite boundary, i.e., following decompression (Grew et al. 2006a). Thus, the original *T-P* estimates for boralsilite formation in the Larsemann Hills could have been too high; 600–700 °C, 3–4 kbar might be more appropriate. These are the conditions estimated for boralsilite formation at Almgjotheii, where andalusite formed

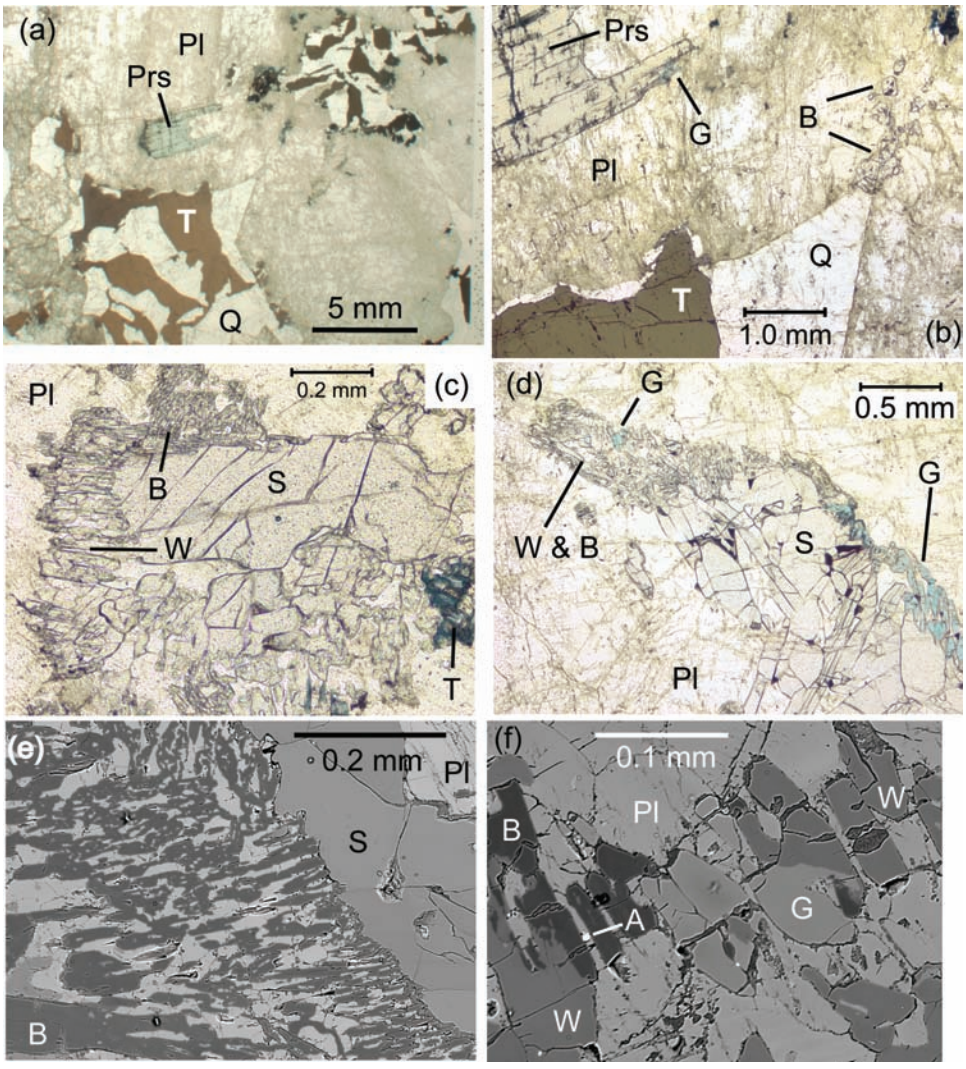

Figure 12. Images of mineral associations in the pegmatite from locality 121102. (**a**) Photomicrograph of graphic tourmaline-quartz intergrowth, prismatine and boralsilite with quartz (not marked) in section 121102C2, plane light. Matrix is plagioclase. (**b**) Enlargement of the center of (**a**), but taken with section in a different orientation, which resulted in a difference in the colors of prismatine and tourmaline. (**c**) Photomicrograph of sillimanite with fringes of werdingite and boralsilite in section 121102B, plane-polarized light. Dark-blue tourmaline is replacing grandidierite. Matrix is plagioclase. (**d**) Photomicrograph of sillimanite with fringes containing werdingite, boralsilite, and grandidierite in section 121102B, plane light. Matrix is plagioclase (**f**); area in back-scattered electron image. (**e**) Back-scattered electron image of a fringe of boralsilite around sillimanite in section 121102B. Matrix is plagioclase with minor quartz (not marked). (**f**) Back-scattered electron image of a portion of fringe in (**d**) showing intergrowth of boralsilite, werdingite and grandidierite, and a tiny grain of apatite. Abbreviations: A = apatite, B = boralsilite, G = grandidierite, Pl = plagioclase, Prs = prismatine, Q = quartz, T = tourmaline, W = werdingite.

early in the boralsilite-bearing pegmatite. The 600–700 °C, 3–4 kbar estimate is consistent with the conditions of synthesis of ordered boralsilite (Fig. 3).

Aluminum-rich borosilicates in granitic pegmatites

Experimental studies have dealt exclusively with the question of tourmaline stability in aluminous granitic systems: tourmaline-group minerals, specifically, schorl-dravite, elbaite, and foitite, are by far the most abundant B minerals in granites and granitic pegmatites derived from anatexis of pelitic and semipeltic rocks. Yet there are examples of granitic pegmatites in which Al-rich borosilicates other than tourmaline are present, in one case to the exclusion of tourmaline (Table 7). Formation of the mineral provisionally identified as "boron-mullite" in metapelites from Mount Stafford also could have involved granitic melt, but this possibility remains too conjectural to consider "boron-mullite" as a constituent of naturally occurring granitic rocks in the present discussion.

What physical-chemical conditions do the three occurrences listed in Table 7 have in common that favored the crystallization of Al-rich borosilicates along side or in lieu of schorl-dravite tourmaline that is so prevalent elsewhere? Boralsilite and

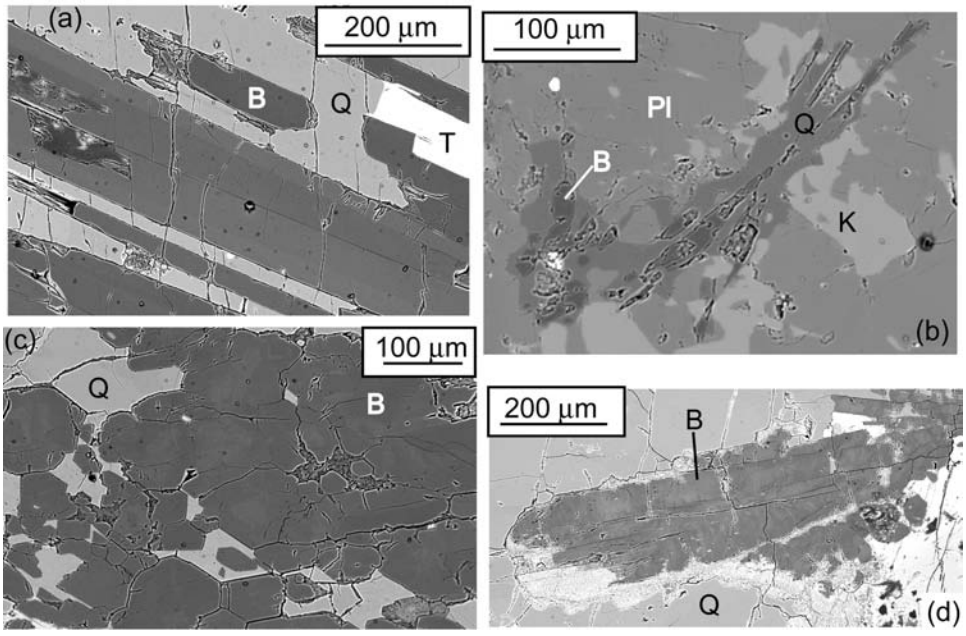

FIGURE 13. Back-scattered electron images of boralsilite in pegmatites from the Larsemann Hills, East Antarctica. (**a**) Boralsilite (type I) shows faint banding parallel to prism length. Sample 010602A. (**b**) Acicular boralsilite (type II) enclosed in quartz surrounded by feldspars. Sample 010205J4. (**c**) Aggregate of boralsilite prisms (type I) showing indistinctly lighter cores. Sample 121502E. (**d**) Aggregate of boralsilite prisms (type 2) showing patchy light areas. Sample 112906B. Abbreviations: B = boralsilite, K = K-feldspar, Pl = plagioclase, Q = quartz, T = tourmaline.

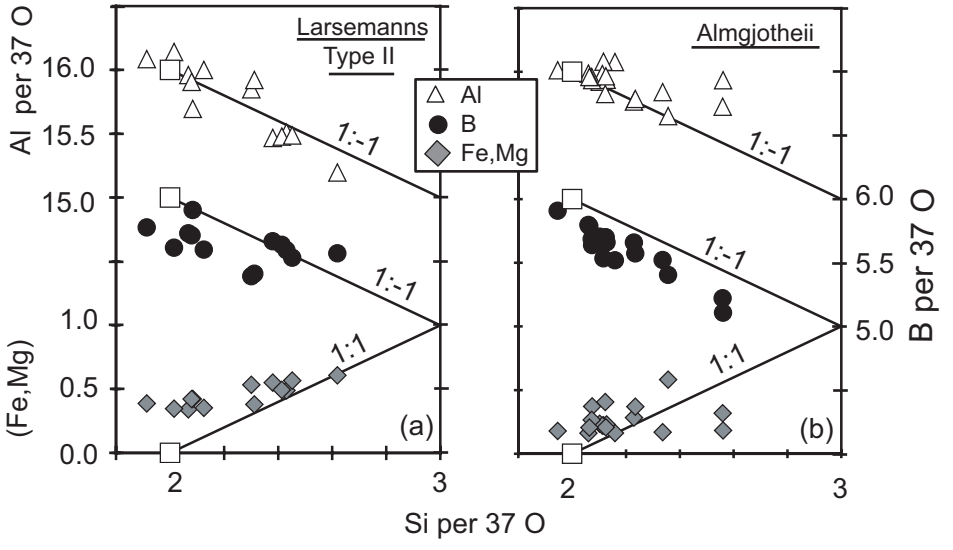

FIGURE 14. (**a**) Compositions of boralsilite in samples 112906B and 010205J4 from the Larsemann Hills (Type II). (**b**) Compositions of boralsilite in samples HE138B2 and HE138B3 from Almgjotheii, Rogaland Complex, SW Norway. Squares indicate ideal composition $Al_{16}B_6Si_2O_{37}$. The lines indicate ideal substitutions. Three Si per 37 O corresponds to 50% solid solution of an ideal werdingite component $(Fe,Mg)_2Al_{14}B_4Si_4O_{37}$.

"boron-mullite" have been synthesized at temperatures readily attained in the Earth's upper crust (Fig. 3), as have werdingite and grandidierite (Werding and Schreyer 1992, 1996), and these four minerals would be expected to be found more often in experiments using peraluminous B-enriched granitic systems, but to date none have been documented conclusively. Acicular phases have been reported in some experimental studies, most recently, an Al-silicate phase in granitic melts synthesized from tourmaline-bearing mixes (Spicer et al. 2004). Chorlton (1973) and Chorlton and Martin (1978) synthesized an acicular phase showing weak blue-green pleochroism by the dry melting of a tourmaline-bearing granite at T = 841–1100 °C and P = 1 bar. Its powder XRD pattern contained up to five lines characteristic of mullite.

TABLE 7. Summary of information on pegmatite containing Al-rich borosilicates

Locality	Tur	Gdd	Bor	Wrd	Dum	Other B	Al_2SiO_5	*T* (°C), *P* (kbar)	Source
Stornes (D_2-D_3), Antarctica	X*, 2nd	X	X	X	2nd	Prs†	Sil, 2nd And	600–700, 3–4	1
Stornes (D_4), Antarctica	X*, 2nd	–	X	–	X, 2nd	–	Sil	600–700, 3–4	–
Almgjotheii, Norway	2nd	X‡	X	X‡	X, 2nd	–	Sil, And	600–700, 3–4	1, 2
Cap Andrahomana, Madagascar	–§	X	–	X	–	–	Sil, 2nd And	600–700, 4	2, 3

Notes: X = present, 2nd = secondary. And = andalusite, Bor = boralsilite, Dum = dumortierite, Gdd = grandidierite, Other B = other borosilicate minerals, Prs = prismatine, Sil = sillimanite, Tur = tourmaline (largely schorl-dravite; 2nd approaches foitite-olenite join), Wrd = werdingite. Principal sources (in addition to this paper): 1 = Grew et al. (1998a); 2 = Grew et al. (1998b); 3 = Lacroix (1904).

* Intergrown with quartz.

† Xenocrystic(?).

‡ In part or entirely as the Fe-dominant analogues.

§ Tourmaline was reported in another pegmatite at Andrahomana (Behier 1961).

Figure 3 shows that the *P*-*T* conditions of synthesis of ordered boralsilite straddle the breakdown of dumortierite in the BASH system and lie within the stability range of dravite in the Na_2O-MgO-BASH system. Werding and Schreyer (1996) emphasized that the thermal breakdown curve of dumortierite is not its true upper stability limit; moreover, as an additional component, Ti could stabilize dumortierite to higher temperatures. The situation with tourmaline is more complex because Fe, Ti, and F would all affect the stability of natural Ti-bearing schorl-dravite. Although schorl-dravite tourmaline commonly breaks down in the amphibolite facies (e.g., Kawakami 2004 shown in Fig. 3), it can persist into the granulite facies (e.g., the Larsemann Hills, Mount Stafford) and it has been synthesized in granitic melts at 800–850 °C, 3.0–3.2 kbar (Spicer et al. 2004). Overall, it is safe to conclude that the stability range of ordered boralsilite overlaps the stability ranges of dumortierite and schorl-dravite, and crystallization of boralsilite (and werdingite) in a peraluminous granitic pegmatite instead of or with tourmaline and dumortierite depends on factors other than pressure and temperature.

One possible explanation for the formation of boralsilite, werdingite, and late-stage grandidierite in pegmatites in the Larsemann Hills could lie in the common association of these minerals with the graphic tourmaline-quartz intergrowths (e.g., Figs. 11c, 11d, and 12b), which could be the products of rapid crystallization due to oversaturation in tourmaline. London et al. (1996) gave this explanation for similar graphic intergrowths of tourmaline and quartz from the Belo Horizonte 1 pegmatite, California. Rapid growth of tourmaline and quartz could have left a residual melt or fluid thoroughly depleted in Fe and Mg, but not B. The fringes of boralsilite, werdingite, and grandidierite in sample 121102B (Figs. 12c–12f) can be interpreted to have resulted from the reaction of these highly evolved melts or fluids with pre-existing sillimanite. Boralsilite prisms isolated from feldspar by quartz (e.g., Grew et al. 1998a, Fig. 1a therein; this paper, Fig. 13b) suggest precipitation of boralsilite with quartz after most feldspar had crystallized. No textures involving boralsilite support the conclusion reached by Grew et al. (1998a) that boralsilite is an "early formed magmatic" mineral.

However, graphic tourmaline-quartz intergrowths are not associated with boralsilite at other localities (e.g., London et al. 1996; Kawakami 2001), and not all Larsemann Hills boralsilite is spatially associated with the graphic tourmaline-quartz intergrowths, e.g., it is also found with grandidierite (Fig. 11e). Graphic tourmaline-quartz intergrowths were not found in the Almgjotheii pegmatite; boralsilite-werdingite intergrowths occur with grandidierite or its Fe-dominant analogue ominelite (Grew et al. 1998b). Grew et al. (1998a) concluded that boralsilite and werdingite in the Almgjotheii pegmatite formed by reactions either between the magmatic minerals grandidierite and dumortierite or between these minerals and fluids, the latter origin analogous to that suggested for sample 121102B from the Larsemann Hills. Werdingite is later than sillimanite and grandidierite in the Cap Andrahomana, Madagascar pegmatite (Grew et al. 1998b). In summary, textural relationships indicate boralsilite and werdingite crystallized from residual melts or fluid remaining after grandidierite crystallized, not only in some Larsemann Hills pegmatites, but also in pegmatites from Almgjotheii and Cap Andrahomana. That is, crystallization of grandidierite, like crystallization of the graphic tourmaline-quartz intergrowths, left remaining melt or fluid depleted in FeO and MgO, but not B, creating conditions favorable for precipitation of boralsilite and werdingite.

Nonetheless, the above explanations leave unanswered the question why boralsilite, werdingite, and grandidierite are such rare minerals in granitic pegmatites. The pegmatite bodies listed in Table 7 contain very few minerals not found in the host rocks except boralsilite, werdingite, and dumortierite (Grew et al. 1998b; Appendix Table 3[1]), and only minor enrichments of Be, Nb, and Ta; i.e., these pegmatites appeared to have undergone relatively little fractionation, but even limited fractionation has resulted in markedly B-enriched pegmatites. This contradiction could be explained if the pegmatites resulted from anatexis of rocks already enriched in B, so that relatively little further fractionation would be necessary to reach unusual B enrichments. We have little evidence for a source of B for the borosilicates in the pegmatites at Almgjotheii and Cap Andrahomana; Grew et al. (1998b) suggested that metasediments rich in tourmaline-bearing graphite could be a source at Almgjotheii, but no tourmaline in the source itself survived metamorphism. In contrast, a B-rich source is evident in the Larsemann Hills. The pegmatites are spatially associated with paragneisses containing up to 10 000 ppm B (Grew et al. 2006b) and abundant prismatine, grandidierite, and tourmaline (Fig. 10), and it is likely that these paragneisses were among the source rocks for the pegmatites. This conclusion is consistent with the presence of what appears to be xenocrystic prismatine (e.g., Figs. 12a and 12b), which could have been entrained from the source of the anatectic melt. Thus, the source rocks are richer in B than typical amphibolite-facies metapelites, in which accessory tourmaline is the primary source of B for tourmaline-bearing pegmatites (e.g., no more than 0.24 vol% tourmaline and 79 ppm B, Kawakami 2001).

Another consideration is the amount of water in the melt: if the residual fluids were drier than in most pegmatites, there would have been less opportunity for metasomatic exchange with the

host rocks and loss of B from the pegmatite, a process that often depletes pegmatites in B (London et al. 1996). The presence of early formed grandidierite instead of tourmaline could indicate low water contents. There is no other compositional factor that obviously would favor the anhydrous phase grandidierite over the hydrous phases of the tourmaline group in a pegmatitic magma. Saturation in MgO and FeO and high activities of both Al_2O_3 and B_2O_3 would also be prerequisites for grandidierite saturation: the activity of grandidierite can be expressed as $K = [Al_{excess}]^3_{melt}[B]_{melt}$, similar to the relation for schorl-dravite tourmaline, $K = [Al_{excess}]^6_{melt}[B]^3_{melt}$ (where Al_{excess} is the portion of Al above that needed for feldspar), in a melt saturated with ferromagnesian phases such as garnet and cordierite (Wolf and London 1997).

The combination of a B-rich source and relatively low water content, together with limited fractionation, resulted in an unusual buildup of B, but not of Li, Be, and other elements normally concentrated in pegmatites. The resulting conditions are favorable in the late stages of pegmatite crystallization for precipitation of boralsilite, werdingite, and grandidierite instead of elbaite and B minerals characteristic of the later stages in more fractionated pegmatites.

Dedication

This paper is dedicated to the memory of Charles V. Guidotti. Over the years as colleagues at the Universities of Wisconsin and Maine, Charlie and Ed Grew commented on each other's manuscripts. Charlie's comments invariably led to improvement, and his enthusiasm was always a source of support. His comments on the draft abstract for the first report of boralsilite (Grew et al. 1996) were no exception: "Minor wording suggestions—If you are not at the number of words limit, try to be a little less terse in your writing. Otherwise looks fine!"

Acknowledgments

We thank the leader, Bob Jones, and other members of the 2003–2004 Australian National Antarctic Research Expedition for logistics support during the summer field season and Doug Thost for information on the whereabouts of the type locality. The thoughtful and constructive reviews of an earlier version of the manuscript by Robert Martin and George Morgan are much appreciated. The fieldwork of C.J.C. and E.S.G. in the Larsemann Hills was supported by Antarctic Science Advisory Committee Project no. 2350. The research of E.S.G. and M.G.Y. was supported by U.S. National Science Foundation grants OPP-0228842 and MRI-0116235 to the University of Maine. I.S.B. acknowledges an Australian Professorial Fellowship and Discovery Grant DP0342473 from the Australian Research Council. G.L.C. acknowledges Australian Research Council grant A39230559 for defraying the logistic expenses for fieldwork at Mount Stafford.

References cited

Angel, R.J. and Prewitt, C.T. (1986) Crystal structure of mullite: A re-examination of the average structure. American Mineralogist, 71, 1476–1482.

Balzar, D. and Ledbetter, H. (1993) Crystal structure and compressibility of 3:2 mullite. American Mineralogist, 78, 1192–1196.

Behier, J. (1961) Travaux minéralogiques. In Rapport Annuel du Service Géologique de Madagascar pour 1961, p. 183–184. Antananarivo, Madagascar.

Buick, I.S., Stevens, G., Hermann, J., and Spicer, E. (2006) The behaviour of boron during LP/HT metamorphism of metapelites, Mt. Stafford, central Australia. Geochimica et Cosmochimica Acta, 70, Issue 18S, A73.

Carson, C.J. and Grew, E.S. (2007) Geology of the Larsemann Hills, Antarctica, First edition (1:25 000 scale map). Geoscience Australia, Canberra.

Carson, C.J., Dirks, P.G.H.M., Hand, M., Sims, J.P., and Wilson C.J.L. (1995) Compressional and extensional tectonics in low-medium pressure granulites from the Larsemann Hills, East Antarctica. Geological Magazine, 132, 151–170.

Chorlton, L.B. (1973) The effect of boron on phase relations in the granite-water system. 95 p. M.S. thesis, McGill University, Montreal, Canada.

Chorlton, L.B. and Martin, R.F. (1978) The effect of boron on the granite solidus. Canadian Mineralogist, 16, 239–244.

Dietzel, A. and Scholze, H. (1955) Untersuchungen im system B_2O_3-Al_2O_3-SiO_2. Glastechnische Berichte, 28, 47–51.

Dušek, M., Petříček, V., Wunschel, M., Dinnebier, R.E., and van Smaalen, S. (2001) Refinement of modulated structures against X-ray powder diffraction data with JANA2000. Journal of Applied Crystallography, 34, 398–404.

Dyar, M.D., Wiedenbeck, M., Robertson, D., Cross, L.R., Delaney, J.S., Ferguson, K., Francis, C.A., Grew, E.S., Guidotti, C.V., Hervig, R.L., Hughes, J.M., Husler, J., Leeman, W., McGuire, A.V., Rhede, D., Rothe, H., Paul, R.L., Richards, I., and Yates, M. (2001) Reference minerals for the microanalysis of light elements. Geostandards Newsletter, 25, 441–463.

Garsche, M., Tillmanns, E., Almen, H., Schneider, H., and Kupčik, V. (1991) Incorporation of chromium into aluminum borate $9Al_2O_3 \cdot 2B_2O_3$ (A_9B_2). European Journal of Mineralogy, 3, 793–808.

Gelsdorf, G., Müller-Hesse, H., and Schwiete, H.-E. (1958) Einlagerungsversuche an synthetischem Mullit und Substitutionsversuche mit Galliumoxyd und Germaniumdioxyd. Teil II. Archiv für das Eisenhüttenwesen, 29(8), 513–519.

Gielisse, P.J.M. and Foster, W.R. (1961) Research on phase equilibria between boron oxides and refractory oxides, including silicon and aluminum oxides, 10 p. Quarterly Progress Report, Ohio State University Research Foundation.

Greenfield, J.E., Clarke, G.L., and White, R.W. (1998) A sequence of partial melting reactions at Mt Stafford, central Australia. Journal of Metamorphic Geology, 16, 363–378.

Grew, E.S., Yates, M.G., Peacor, D.R., Rouse, R.C., McGee, J.J., Huijsmans, J.P.P., and Thost, D.E. (1996) A new borosilicate mineral with a structure derivative to that of sillimanite and its paragenesis in pegmatites. Geological Society of America Abstracts with Programs, 28, A-102

Grew, E.S., McGee, J.J., Yates, M.G., Peacor, D.R., Rouse, R.C., Huijsmans, J.P.P., Shearer, C.K., Wiedenbeck, M., Thost, D.E., and Su, S.-C. (1998a) Boralsilite ($Al_{16}B_6Si_2O_{37}$): A new mineral related to sillimanite from pegmatites in granulite-facies rocks. American Mineralogist, 83, 638–651.

Grew, E.S., Yates, M.G., Huijsmans, J.P.P., McGee, J.J., Shearer, C.K., Wiedenbeck, M., and Rouse, R.C. (1998b) Werdingite, a borosilicate new to granitic pegmatites. Canadian Mineralogist, 36, 399–414.

Grew, E.S., Armbruster, T., Medenbach, O., Yates, M.G., and Carson, C.J. (2006a) Stornesite-(Y), $(Y, Ca)\square_2Na_6(Ca,Na)_8(Mg,Fe)_{43}(PO_4)_{36}$, the first terrestrial Mg-dominant member of the fillowite group, from granulite-facies paragneiss in the Larsemann Hills, Prydz Bay, East Antarctica. American Mineralogist, 91, 1412–1424.

Grew, E.S., Christy, A.G., and Carson, C.J. (2006b) A boron-enriched province in granulite-facies rocks, Larsemann Hills, Prydz Bay, Antarctica. Geochimica et Cosmochimica Acta, 70, Issue 18S, A217.

Hill, R.J. and Flack, H.D. (1987) The use of the Durban-Watson d-statistic in Rietveld analysis. Journal of Applied Crystallography, 20, 356–361.

Ihara, M., Imai, K., Fukunaga, J., and Yoshida, N. (1980) Crystal structure of boroaluminate, $9Al_2O_3 \cdot 2B_2O_3$. Yogyo-Kyokai-Shi, 88(2), 77–84 (in Japanese with English abstract).

Kawakami, T. (2001) Boron depletion controlled by the breakdown of tourmaline in the migmatite zone of the Aoyama area, Ryoke metamorphic belt, southwestern Japan. Canadian Mineralogist, 39, 1529–1546.

——— (2004) Tourmaline and boron as indicators of the presence, segregation and extraction of melt in pelitic migmatites: examples from the Ryoke metamorphic belt, SW Japan. Transactions of the Royal Society of Edinburgh: Earth Sciences, 95, 111–123.

Krosse, S. (1995) Hochdrucksynthese, Stabilität und Eigenschaften der Borsilikate Dravit und Kornerupin sowie Darstellung und Stabilitätsverhalten eines neuen Mg-Al-borates, 131 p. Ph.D. thesis, Ruhr-Universität, Bochum.

Lacroix, A. (1904) Sur la grandidiérite. Bulletin de la Société française de Minéralogie, 27, 259–265.

Letort, Y. (1952) Contribution à l'étude de la synthèse de la mullite. Transactions of the International Ceramic Congress, p. 19–32.

London, D., Morgan, G.B. IV, and Wolf, M.B. (1996) Boron in granitic rocks and their contact aureoles. In E.S. Grew and L.M. Anovitz, Eds., Boron: Mineralogy, Petrology and Geochemistry, 33, p. 299–330. Reviews in Mineralogy, Mineralogical Society of America, Chantilly, Virginia.

Mazza, D., Vallino, M., and Busca, G. (1992) Mullite-type structures in the systems Al_2O_3-Me_2O (Me = Na, K) and Al_2O_3-B_2O_3. Journal of the American Ceramic Society, 75, 1929–1934.

McGee, J.J. and Anovitz, L.M. (1996) Electron probe microanalysis of geologic materials for boron. In E.S. Grew and L.M. Anovitz, Eds., Boron: Mineralogy, Petrology and Geochemistry, 33, p. 771–788. Reviews in Mineralogy, Mineralogical Society of America, Chantilly, Virginia.

Merlet, C. (1994) An accurate computer correction program for quantitative electron-probe microanalysis. Mikrochimica Acta, 114, 363–376.

Pattison, D.R.M. (1992) Stability of andalusite and sillimanite and the Al_2SiO_5 triple point: Constraints from the Ballachulish aureole, Scotland. Journal of Geology, 100, 423–446.

Peacor, D.R., Rouse, R.C., and Grew, E.S. (1999) Crystal structure of boralsilite and its relation to a family of boroaluminosilicates, sillimanite, and andalusite. American Mineralogist, 84, 1152–1161.

Petříček, V. and Dušek, M. (2000) Jana2000. Structure Determination. Software Programs. Institute of Physics, Prague, Czech Republic.

Pöter, B., Werding, G., Schreyer, W., and Bernhardt, H.J. (1998) Synthesis and properties of the new borosilicate mineral boralsilite. Berichte der Deutschen Mineralogischen Gesellschaft, 1, 220.

Rietveld, H.M. (1969) A profile refinement method for nuclear and magnetic structures. Journal of Applied Crystallography, 2, 65–71.

Robbins, C.R. and Yoder, H.S., Jr. (1962) Stability relations of dravite, a tourmaline. Year Book, Carnegie Institution of Washington, 61, 106–107.

Scholze, H. (1956) Über Aluminiumborate. Zeitschrift für anorgische allgemeine Chemie, 284, 272–277.

Sokolova, Ye.V., Azizov, A.V., Simonov, M.A., Leonyuk, N.I., and Belov, N.V. (1978) Crystal structure of synthetic ortho-3-borate $Al_5(BO_3)O_6$. Doklady Akademii Nauk SSSR, 243, 655–658 (in Russian).

Sorbier, L., Rosenberg, E., and Merlet, C. (2004) Microanalysis of porous materials. Microscopy and Microanalysis, 10, 745–752.

Spicer, E.M., Stevens, G., and Buick, I.S. (2004) The low-pressure partial-melting behaviour of natural boron-bearing metapelites from the Mt. Stafford area, central Australia. Contributions to Mineralogy and Petrology, 148, 160–179.

Stachowiak, A. and Schreyer, W. (1998) Synthesis, stability and breakdown products of the hydroxyl end-member of jeremejevite in the system Al_2O_3-B_2O_3-H_2O. European Journal of Mineralogy, 10, 875–888.

Vernon, R.H., Clarke, G.L., and Collins, W.J. (1990) Local, mid-crustal granulite facies metamorphism and melting: an example in the Mount Stafford area, central Australia. In J.R. Ashworth and M. Brown, Eds., High-temperature metamorphism and crustal anatexis, p. 272–319. Unwin Hyman, London.

Werding, G. and Schreyer, W. (1984) Alkali-free tourmaline in the system MgO-Al_2O_3-B_2O_3-SiO_2-H_2O. Geochimica et Cosmochimica Acta, 48, 1331–1344.

——— (1992) Synthesis and stability of werdingite, a new phase in the system MgO-Al_2O_3-B_2O_3-SiO_2 (MABS), and another new phase in the ABS-system. European Journal of Mineralogy, 4, 193–207

——— (1996) Experimental studies on borosilicates and selected borates. In E.S. Grew and L.M. Anovitz, Eds., Boron: Mineralogy, Petrology and Geochemistry, 33, p. 117–163. Reviews in Mineralogy, Mineralogical Society of America, Chantilly, Virginia.

White, R.W., Powell, R., and Clarke, G.L. (2003) Prograde metamorphic assemblage evolution during partial melting of metasedimentary rocks at low pressures: migmatites from Mt Stafford, Central Australia. Journal of Petrology, 44, 1937–1960.

Wodara, U. and Schreyer, W. (2001) X-site vacant Al-tourmaline: a new synthetic end-member. European Journal of Mineralogy, 13, 521–532.

Wolf, M.B. and London, D. (1997) Boron in granitic magmas: stability of tourmaline in equilibrium with biotite and cordierite. Contributions to Mineralogy and Petrology, 130, 12–30.

Manuscript received January 19, 2007
Manuscript accepted July 20, 2007
Manuscript handled by Francesco Sassi